Computational Biomechanics of the Lumbar Spine: A Study of Lower Back Pain (LBP) Based on Muscle Strength

By

Saadia Talay

00000322057

Supervisor

Dr Zartasha Mustansar

Department of Computational Science and Engineering, School of Interdisciplinary Engineering and Sciences (SINES), National University of Sciences and Technology (NUST)

Islamabad, Pakistan

December 2022

Computational Biomechanics of the Lumbar Spine: A Study of Lower Back Pain (LBP) Based on Muscle Strength

By

Saadia Talay

00000322057

Supervisor

Dr Zartasha Mustansar

A thesis submitted in conformity with the requirements for the degree of *Master of Science* in Computational Science and Engineering

School of Interdisciplinary Engineering and Sciences (SINES),
National University of Sciences and Technology (NUST)

Islamabad, Pakistan

December 2022

Annex A to NUST Letter No. 0972/102/Exams/Thesis-Cert dated 23 Dec 16.

Thesis Acceptance Certificate

Certified that final copy of MS/MPhil thesis written by Mr/Ms Saadia Talay, Registration No. 00000322057 of **SINES** has been vetted by undersigned, found complete in all aspects as per NUST Statutes/Regulations, is free of plagiarism, errors, and mistakes and is accepted as partial fulfilment for award of MS/MPhil degree. It is further certified that necessary amendments as pointed out by GEC members of the scholar have also been incorporated in the said thesis.

Signature with stamp: _____

Name of Supervisor: _____

Date: _____

Signature of HoD with stamp: _____

Date: _____

Countersign by

Signature (Dean/Principal): _____

Date: _____

Declaration

I, *Saadia Talay,* declare that this thesis titled "Computational Biomechanics of the Lumbar Spine: A Study of Lower Back Pain (LBP) Based on Muscle Strength" and the work presented in it are my own and has been generated by me as a result of my own original research.

I confirm that:

1. This work was done wholly or mainly while in candidature for a Master of Science degree at NUST
2. Where any part of this thesis has previously been submitted for a degree or any other qualification at NUST or any other institution, this has been clearly stated
3. Where I have consulted the published work of others, this is always clearly attributed
4. Where I have quoted from the work of others, the source is always given. With the exception of such quotations, this thesis is entirely my own work
5. I have acknowledged all main sources of help
6. Where the thesis is based on work done by myself jointly with others, I have made clear exactly what was done by others and what I have contributed myself

_____

Saadia Talay,
00000322057

Copyright Notice

This thesis is dedicated to finding a path for scientific research

Abstract

Chronic Low Back Pain afflicts a large number of people worldwide. The lower spine is comprised of lumbar vertebrae with intervertebral discs, and a fused sacrum that articulates with the iliac bones. The whole assembly is stabilized by large synergistic and antagonist groups of muscles. A dysfunction or abnormality in any of these structures could lead to instability and disturbed load distribution that could lead to pain. Gluteus maximus is the largest muscle in the human body contributing to the stability of the pelvis, hip and knee during gait and other activities. The present study is focused on determining effects of variation in strength of the gluteus maximus on the compressive load exerted on the sacroiliac joint. Additionally, the effects on pelvic tilt, hip and knee loads, and angles with the change in gluteus maximus strength were also explored.

Our results for a single gait cycle showed maximum anterior pelvic tilt with an atrophied and hypertrophied gluteus maximus as 0.2308 and 0.1900 radians respectively as compared to a maximum anterior pelvic tilt of 0.1994 in the unaltered model. This indicates a noticeable variation in pelvic tilt based on varying strength of the gluteus maximus while there were small changes in the hip and knee loads. It was also observed that the hamstrings play a compensatory role in stabilizing the knee and the hip with minimal changes in their angles and loading for the same gait cycle.

Acknowledgements

In the name of Allah, the all-knowing and the most perfect guide

I am thankful to Dr. Zartasha Mustansar for taking me under her wing and providing me with opportunities that refined me as a researcher and made me into a well-rounded professional. I would also like to thank Dr. Rehan Zafar Paracha for his valuable feedback and downpour of encouragement. Thanks to Dr. Absaar Ul Jabbar for reviewing my study and helping me refine it. I would like to extend my thanks to the principal, Dr. Hammad Cheema and the HOD, Dr. Mian Ilyas Ahmad for creating a conducive environment for learning and research.

This work wouldn't have been possible without my father who was my constant brainstorming buddy. He pushed and guided me at each stage of the project from the inception till its conclusion, constantly providing me with his valuable insights, feedback and ideas.

A very special thanks to my late uncle, Dr. Sohail Qureshi, and his son, Abdullah Sohail Qureshi, for technically guiding me, helping me, and motivating me throughout the project.

I would like to thank my mother for being a pillar of support throughout my studies; my brother, Adil for engaging me in discussions that lead to new ideas; my sister for her never wavering trust and support; and lastly but very importantly, my younger brother, Dr. Asim, for helping me with the medical terminology and aspects of this study.

Finally, I would like to express my gratitude to my loving husband and his amazing mother for providing me with a suitable environment to continue my research and their constant support and encouragement to fulfil my ambitions and reach for my goals.

Table of Contents

List of Tables

List of Figures

List of Abbreviations

ALS	Amyotrophic Lateral Sclerosis
CNS	Central Nervous System
CC	Contractile Component
CSA	Cross Sectional Area
DMS	Duchenne muscular dystrophy
FA	Force Activation
FL	Force Length
FV	Force Velocity
GMAX	Gluteus Maximus
JRF	Joint Reaction Force
PEC	Parallel Elastic Component
SEC	Series Elastic Component
SA	Stimulation Activation

Research Contributions

- Compressive back load shows a minor change with variation in gluteus maximus strength
- Anterior pelvic tilt shows a noticeable increase with atrophy of GMAX
- Hip and Knee angles are maintained at the expense of load
- Hamstrings play a compensatory role in case of GMAX deficiency
- Persistent deficiencies could manifest in the form of crippling disabilities
- Proved the utility of the plantarflexor weakness model and SCONE for atrophy and hypertrophy of GMAX

CHAPTER 1

INTRODUCTION

1.1 Background

Lower backpain (LBP) is a musculoskeletal problem that affects the society at large. It has an adverse effect on functional mobility; it prevents patients from being able to perform routine activities while also incurring huge socioeconomic costs. It is thus classified as one of the major global public health problems [1].

High spinal loading as well as muscle disuse atrophy are some of the common causes of lower back pain. In Pakistan, a major portion of the blue collared jobs require high loading manual tasks that involve awkward postures. On the other hand, a major portion of the white collared jobs require sitting postures for long hours at a stretch. This could be a probable cause of abnormal stresses on the spine. In addition, most people are also prone to muscle atrophy due to a sedentary lifestyle.

It is found that the prevalence of LBP increases linearly in the third decade of life and is more prevalent in females than in males [2, 3]. LBP was defined as pain that lasts for at least one day (with/without pain referred into one or both lower limbs) in the area on the posterior aspect of the body from the lower margin of the 12th ribs to the lower gluteal folds [4].

Until recently, muscles were not given due importance in relation to LBP. However, in the last decade, scientists have been studying the interaction between the atrophy of specific muscles, LBP and spinal pathology.

The gluteus maximus is one of the largest muscles in the body responsible for movement of the hips and knees and maintaining an upright posture. It extends from the lower back through an aponeurosis to the femur. Any disorder or injury affecting the muscle would lead to a change in the force distribution in the musculoskeletal structures surrounding it.

1.2 Research Objective

The aim of this study is to analyse the effect of of major muscle, for example, the gluteus maximus muscle on the lumbosacral spine. We want to use predictive simulation with varying gluteus maximus strengths to compute the loads on the back as well as the hip and the knee. We would also like to see the pelvic tilt and hip and knee angles along the gait cycle. Moreover, we would like to investigate the effect of changing gluteus maximus strength on the force exerted by the hamstrings.

This dissertation contains a chapter of literature review where important aspects related to the study are described. This is followed by the methodology where the approach to the study is discussed in detail. The results chapter detail the outcomes of the methods. Lastly, the conclusion and future work discuss the significance of the study and subsequent studies that can be performed to better the current study, to further build upon it, or tangent studies that can be developed.

CHAPTER 2

LITERATURE REVIEW

This chapter discusses some of the important topics related to the study. We justify the importance of posture and its relation to the spine, followed by a detailed explanation of the anatomy of the lower back. This is followed by a description of the gluteus maximus and its relation to lower back pain. We discuss muscle modelling and its different components. Lastly, we list some of the present models available for musculoskeletal modelling studies similar to the current study,

2.1 Posture Biomechanics

Posture can be defined as the arrangement of the parts of the body with respect to each other. Knowledge of the mechanics of the body and its response to stresses and strains enables one to correct faulty postures. Proper alignment and muscle balance results in good body mechanics and movement. A non-optimal usage, either under or over usage, of body structures (muscles/bones) and their function is likely to lead to disproportionate force distribution on joints, bones, muscles, and ligaments. Continual orientation in incorrect postures may result in discomfort, pain, and even disability [5].

Cumulative effects of minor but repetitive stresses can result in the same kind of results as those with sudden and severe stresses. Mobility and flexibility as well as muscle stiffness and tightness are factors that contribute to the relationship between pain and posture. Abnormal human postures in modern, everyday life as well as certain physically demanding jobs result in undue postures [5].

2.2 The Spine

The human spine acts as a scaffold for the entire body helping to maintain an erect posture while bearing the load of the upper body. It is made up of 24 rigid vertebrae separated by intervertebral discs (Figure 2.1). This large number of subcomponents provides a certain degree of flexibility to the spine and allows for a wide range of static and dynamic postures. Any changes in the shape of the spine affects the stresses and strains on the spinal tissues as well as its supporting musculature and vice versa [6]. Excessive forces or moments along the length of the spine may result in spinal trauma, disc herniation, and/or spinal deformities [7].

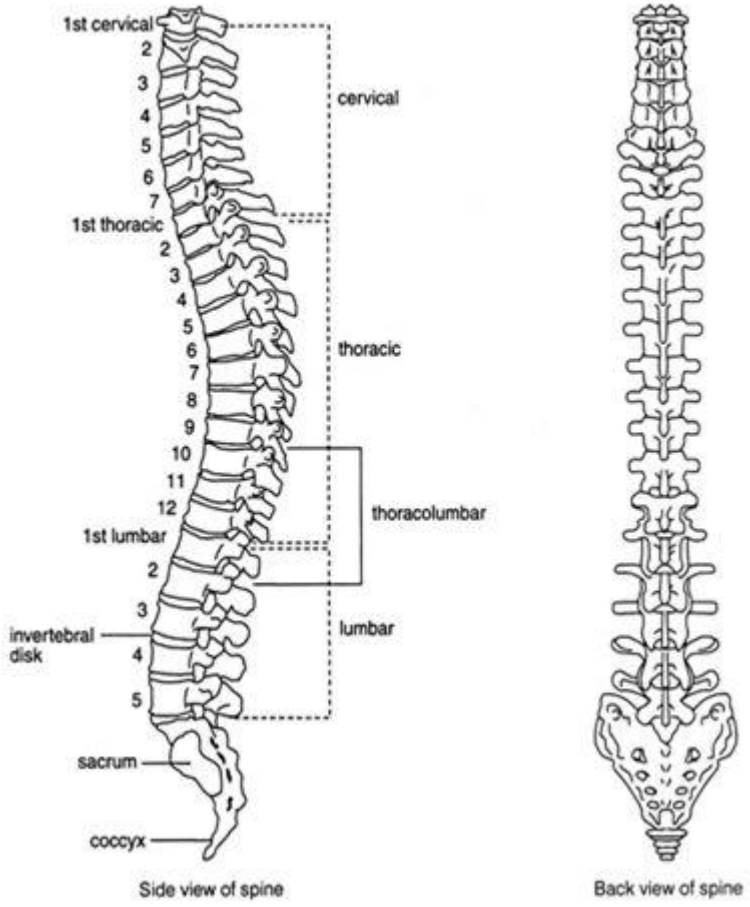

Figure 2.1: The human spine contains 7 cervical vertebrae, 12 thoracic vertebrae, and 5 lumbar vertebrae followed by the sacrum and the coccyx [8]

For the spine to function properly, it must be in a proper orientation with the pelvis and hip joints [7]. The spine is surrounded by an intricate and complex structure of muscles and ligaments which move and compensate in various ways with each spinal movement. Computing each of these movements along with the forces, stresses and strains is a challenging task. However, these may be approximated using detailed mathematical models whose aim is to achieve mechanical equilibrium. The models may be finite element models, or rigid body dynamic models. These can provide important insights to the relationship between forces, stresses, and strains. However, they require experimental validation which can be physically and temporally demanding [7]. Moreover, at best these are approximations and cannot represent accurate in vivo results.

The intrinsic shape of the lumbar spine varies between individuals with each individual maintaining an element of their default shape despite postural changes [6]. Arjmand and Shirazi-Adl [9] combined in vivo measurements and model studies of to investigate the effect of changes in lumbar posture during static lifting tasks. They measured the kinematics of the spine and surface EMG activity of selected muscles of the subjects under different forward trunk flexion angles and lumbar postures. These were used to compute muscle forces, internal loads, and system stability with and without an external load. They concluded that muscle forces and internal spinal loads were significantly affected because of alterations in the lumbar lordosis in lifting tasks.

2.3 Anatomy of the Lower Back

The lower back consists of five lumbar vertebrae followed by five sacral vertebrae that are fused together. The sacrum is connected to the ilium on either side, the large part of the hip bone, through the two sacroiliac joints at the posterior aspect of the pelvis (figure 2.2).

One of the factors in nonspecific chronic low back pain is instability of pelvis, sacroiliac joint, and lower spine. A number of muscles are involved in stabilizing the pelvis, the sacroiliac joint, and the lower back (lumbar spine). Amongst them is the gluteus

maximus, and the gluteus medius [10]. The forces generated by gluteus maximus act directly on sacroiliac joint and indirectly on the lumbar spine through the thoracolumbar facia. Any alteration in the muscle mass/function would affect the balance of forces on the sacroiliac joint and the lumbar spine and could lead to dysfunction/pain in the lower back.

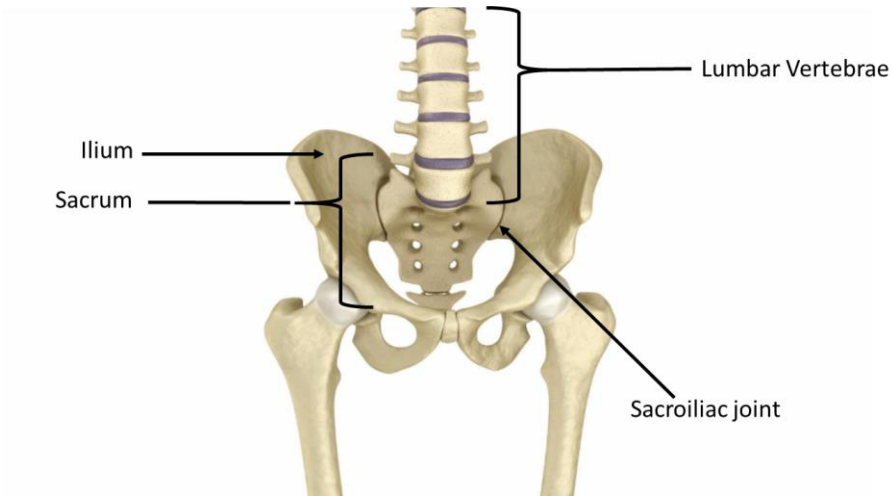

Figure 2.2: The pelvis is connected to the spine through the sides of the sacrum [11]

2.3.1 Gluteus Medius and Gluteus Minimus

The gluteus medius along with the gluteus minimus are the two primary hip abductors and they play an important role in stabilizing the pelvis on the femur during gait. The anterior portions of both of these contribute to the forward contralateral rotation of the pelvis [12]. The gluteus medius completely covers the gluteus minimus. They lie inferior to the anterior part of the iliac crest in a slight depression under the gluteus maximus [13]. Paralysis of these muscles have serious effects on the patient's ability to tilt the pelvis during gait [10].

2.3.2 Gluteus Maximus

The gluteus maximus is the largest muscle in the body and is the most superficial out of the muscles of that region (Figure 2.3) [10, 14]. It has a broad origin and therefore,

it is connected to multiple areas of the posterior pelvic region. The origins include the posterior gluteal line of the ilium and the rough area of the bone, including the crest, immediately above and behind it; from the aponeurosis of erector spinae; the dorsal surface of the lower part of the sacrum and the side of the coccyx; the sacrotuberous ligament; and the fascia (gluteal aponeurosis) which covers gluteus medius. There may be additional slips from the lumbar aponeurosis or ischial tuberosity. Acting from its distal attachment, it may prevent the forward momentum of the trunk from producing flexion at the supporting hip during bipedal gait. However, it acts with the hamstrings in raising the trunk after stooping, by rotating the pelvis backwards on the head of the femur [13].

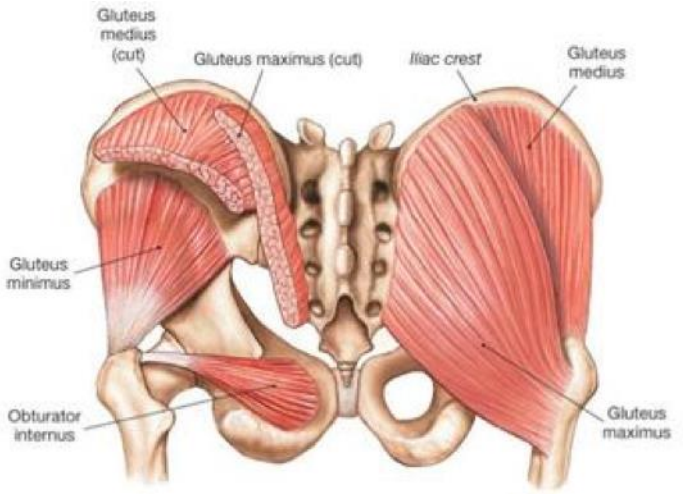

Figure 2.3: The Gluteus maximus, gluteus medius, and the gluteus minimus [15]

2.3.3 Erector spinae aponeurosis

A portion of the uppermost fibres of gluteus maximus arise from the dorsal surface of the inferolateral corner of the erector spinae aponeurosis. The thoracic and lumbar components of erector spinae are powerful extensors of the vertebral column. Acting concentrically and bilaterally they can extend the thoracic and lumbar spines whereas acting unilaterally they can laterally flex the trunk. However, more commonly, erector spinae act eccentrically [13].

2.3.4 Thoracolumbar Fascia

The thoracolumbar (lumbodorsal) fascia covers the deep muscles of the back and the trunk. In the lumbar region, the thoracolumbar fascia is in three layers. The middle and posterior layers enclose the erector spinae muscles and are attached to the lumbar and sacral vertebrae and the interspinous ligaments on one hand and to the iliac crest on the other. The thoracolumbar fascia is continuous with the fascia of the gluteus maximus and can thus putatively play an important role in load transfer between the trunk and the limbs [13].

2.4 Clinical Relevance of the Gluteus Maximus

The GMAX works with other muscles and muscle groups to serve an array of functions for optimal movement and athletic performance. In case of muscle dysfunction, the synergistic properties of the human body causes surrounding musculoskeletal structures to compensate to allow similar movements. This compensation may ultimately lead to overload or acute injuries due to excessive force of certain joints and muscles [16, 17].

The GMAX acts as a local stabilizer providing stability to the lower back via the erector spinae and the thoracolumbar fascia, the sacroiliac joint by bracing and compression, the lumbosacral region via the psoas major, the femoral head via translation, and the knee through its attachment into the iliotibial band [18].

The muscle also acts as a global stabilizer to control range of motion across three planes of motion. It functions with the other gluteal muscles to stabilize the hip preventing trunk forward lean and trunk rotation. It acts to stabilize the pelvis during single leg stance by preventing adduction and internal rotation of the femur [18].

The GMAX produces large amounts of force and power acting as a global mobilizer causing hip extension and external rotation of the femur, while the superior fibers act to produce hip abduction torque, and the inferior fibers act to produce hip adduction torque [18].

The weakness of the GMAX has been implicated in numerous injury types such as anterior knee pain [19], low back pain [20, 21], hamstring strains [22], and femoral acetabular impingement syndrome [23]. This indicates that the weakness/dysfunction of the GMAX may be a contributing risk factor to or the result of injury.

Prolonged sitting postures reduces GMAX activation causing atrophy and weakness with time [24, 25]. This weakness of the GMAX is thought to increased reliance on the secondary hip extensor muscles, such as the hamstrings and hip adductors to produce hip extension torque [26, 27], clinically referred to as 'synergistic dominance' [26]. This is due to the human body utilizing the path of least resistance, which refers to utilizing the most energy efficient motor pattern regardless whether this uses what would be considered the primary agonist for that role [26]. This would increase the relative demands placed upon the synergist muscles and potentially contribute to pain and strain injuries associated with these muscles.

Altered posture of the pelvis can reduce its stabilizing capacity influence due to the length-tension relationship of GM [28]. Associated with hip flexor tightness and local core weakness is an anterior tilted pelvis, which elongates the GMAX and places the muscle in a mechanically disadvantaged position [29].

2.5 Correlation of the strength of Gluteus Maximus with Lower Back Pain

A study conducted in 2016 by Amabile et al. reported that there exists a statistically significant negative correlation between the cross sectional area (CSA) of the gluteus maximus and lower back pain in women between the ages of 40 and 69 [14]. Jeong et al. noted that including gluteus strengthening exercises in a regimen along with lumbar segmental stabilization exercises was more effective in treating lower back pain than just lumbar segmental stabilization exercises alone [30]. Skorupska et al. confirmed in a study that 50% of lower back related leg pain had a smaller volume of the gluteus maximus [31].

2.6 Computer Simulation of Human Movement

Modelling is a powerful yet very limited tool. It allows for quick and cost-effective methods to test systems and products in a variety of ways. However, models only provide near approximations of the actual results and thus, to properly use a model, their limitations must be recognized.

Systems can either be modelled physically or mathematically. Physical modelling includes scaled models of the real system which is then tested according to its usage. These systems require time, money, and resources to develop and can often only be used once. In behavioural or mathematical modelling, the problem is represented as a set of equations which can be solved, often using a computer, to obtain the solution to a particular question.

The process of modelling begins with a research question according to which the model is constructed. The model is then iteratively refined and improved until it can make predictions which answer our specific research question and/or provide new understandings of the system being studied. The results of the model are evaluated against experimental data to ensure their validity. If the results obtained are unrealistic, it must be determined whether the problem is in the model or the way the simulation is being operated.

A rule of thumb in mathematical of modelling is to simplify the system as much as possible by limiting the number of components. This ensures a less tedious and faster solution. Biomechanists use the same approach by simplifying the human body and in many places, grouping the net effects of multiple bones, joints, and muscles.

The human body is incredibly complex with inherent limitations and variability across subjects as well as within the same subject. Fatigue, mental health, and food all play a role into a how a subject will perform in a specific trial. Moreover, some experiments possess safety risks and would be unethical to perform on live subjects. Computer models allow for a controlled environment with no safety risks. Further, simulations allow for experimental conditions that exceed practical limits. Single parameters can be changed within the model to study the effect of change in one single unit on the entire system. This is impractical in real subjects since the complex organ systems in

the body adapt and compensate for an imbalance of forces making it difficult to discern between the cause and effect. Optimal solutions can be computed using simulations for clinical and athletic purposes.

Biomechanical modelling requires an understanding and a proper implementation of multiple technical areas which include, but are not limited to, anatomy and biology, mathematical techniques, and computer programming [32].

2.6.1 Free-body Diagrams

The first step in developing a simulation is to create a free body diagram of the mechanical model. The equations of motion are then derived for that model and a program is written to obtain a numerical solution for those equations. The boundary conditions are determined, and the program is implemented. The model kinematics and, in some cases, kinetics are obtained. This data is then interpreted and compared with experimental data to ensure validity.

The free body diagram allows the researcher to understand the number of components, the types of motion and the degrees of freedom (DOF) of each component of the system. It also allows for the researcher to notice and perceive any parts that can be further simplified [32].

2.6.2 Numerical Techniques

To represent the motion of the system mathematically, several numerical techniques can be applied. Differential equations consider every kinetic factor that affects the movement of a particular segment. This includes the muscle, joint and frictional forces as well as gravity. As the complexity of the model increases so does the complexity of the differential equations governing it.

Numerical solution technique is a method in which the differential equations are iteratively solved to estimate the change in the position of the body over small periods of time. Known values for the starting positions and velocities define the initial energy of the system. These are then used in the differential equations to compute a new set of

positions and velocities. This process is iteratively repeated till a desired end goal is met. This is called as forward simulation, forward solution, or numerical integration [32].

2.6.3 Closed loop or open loop

When a system obtains information from its surroundings as feedback, and uses this information to alter its processes, it is known as a closed loop system. Conversely, an open loop system continues to work in a preprogramed manner regardless of the changes in its environment [32].

2.6.4 Limitations of Computer Models

As powerful and beneficial as simulations are, even the most sophisticated models are limited in their functionality. The complexity of the human systems and their environment makes it inevitable to approximate and assume certain quantities leading to inexact results. Mathematical solutions of such complex systems are bound to be subjected to numerical imperfections. Consequently, the results of these models should be interpreted with caution [32].

2.7 Muscles and Modeling

Inverse dynamics uses kinematics to determine the kinetic properties of a moving body. It estimates the resultant moment at a joint that arise in response to the sum of all individual muscle forces, but it cannot resolve the joint into individual muscular forces.

Forward dynamics uses the applied forces driving a mathematically modeled system to calculate the kinematic trajectories of the system. This approach allows scientists to study how difference in forces of a specific individual results in difference in movement patterns [32]. These are illustrated in Figure 2.4.

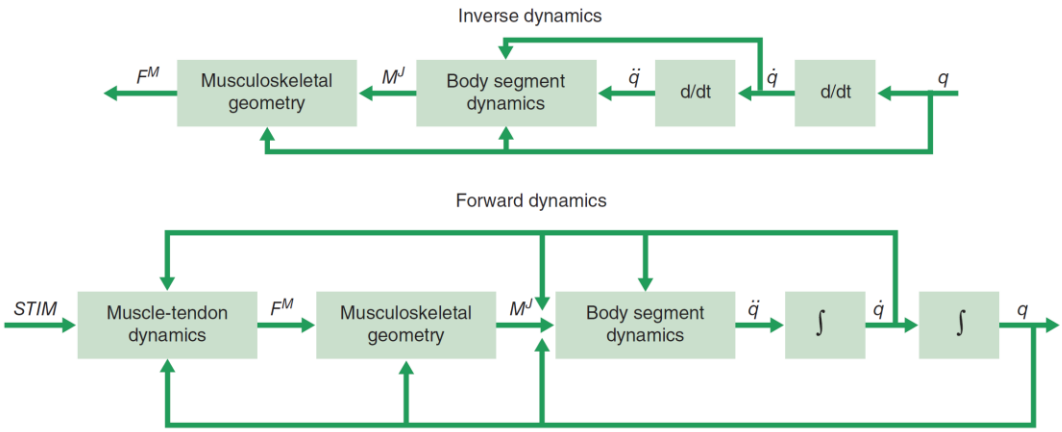

Figure 2.4: Inverse dynamics vs forward dynamics [32].

2.7.1 Electrophysiological Signals

Muscular force is produced due to the central nervous system (CNS) sending an electrical impulse to the synapses in the muscle fibers. Ionic activity at the synapse generates muscle fiber action potential (AP) producing a muscular force, and thereby movement of the associated body part.

A motor unit is the combined structure of a single motoneuron, and the multiple muscle fibers innervated by that neuron. The initiation of muscular activity begins with the recruitment of smaller motor units. Larger motor units are successively recruited as the force requirement increases. The frequency at which the motor units are discharged also determines the amount of force that is produced; as the firing rate of the motor unit increases, the muscular force increases correspondingly.

The contractile function of a skeletal muscle is based on anatomical structure that can be described at the level of the whole muscle, muscle fascicles, muscle fibers or even individual sarcomeres. Sarcomeres are made up of the contractile proteins actin and myosin which respectively form thick and thin filaments. The coupling of these filaments produces muscular force which enables skeletal movement.

A nervous input may cause a muscle to shorten, lengthen, or remain at a constant length depending on the internal and external forces acting on the skeleton. The relationship

between the nervous signal and muscular force is not linear. Rather, the amount of muscular force produced differs according to the type of stimulation and experimental conditions [32].

2.7.2 The Hill Muscle Model [33]

A.V Hill developed a model that could represent muscle function. The basic Hill model consists of 3 components that together represent the model behavior:

1. The contractile component (CC)
2. The series elastic component (SEC)
3. The parallel elastic component (PEC)

These are illustrated in Figure 2.5

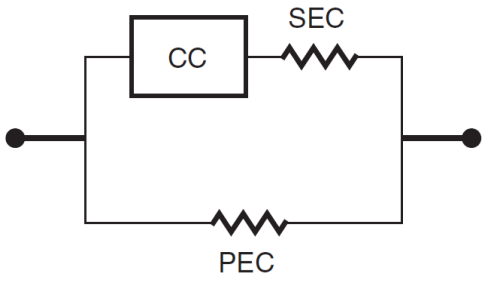

Figure 2.5: The hill muscle model consisting of the contractile component along with the series elastic component and the parallel elastic components [32]

2.7.2.1 The Contractile Component

The CC is the active element of the model which turns nervous signal into force. The amount of force depends on the mechanical characteristics of the CC which are as follows:

1. Stimulation Activation (SA)
   SA is concerned with the muscles' intrinsic force properties. The stimulation is the input, which causes a physiological excitation – contraction coupling process, resulting in an output known as activation.

Activation is the state in which force can be produced and not the actual force level. The actual force level depends on activation as well as the kinematic state of the CC.

2. Force Activation (FA)

   FA is a conceptual relation that converts the level of activation to an actual force level expressed in either newtons or as a percentage of a muscle's maximal force. Therefore, the FA relation is direct and linear.

3. Force Velocity (FV)

   FV expresses the influence of the CC on force production. This is mathematically expressed by the Hill equation for a rectangular hyperbola

$$(P + a)(v + b) = (P_o + a)b \tag{2.1}$$

where

P is the CC force at an instant in time

v is the CC velocity at an instant in time

P_o is the force level the CC would attain at that instant if it were isometric

a and b are muscular dynamic constants representing energy liberation

This Hill equation only refers to isometric or concentric CC velocities. The equation must be modified to include CC eccentric (lengthening) conditions. The force velocity relationship is shown in Figure 2.6.

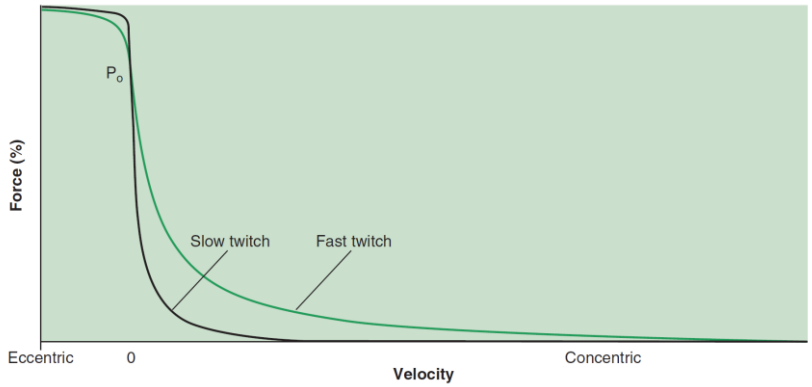

Figure 2.6: The force velocity relationship [32]

4. Force Length (FL)

   FL expresses the dependance of the isometric force production on the CC length.

   FL expresses the dependance of the isometric force production on the CC length. The force is greatest at intermediate CC lengths and decreases as the CC either lengthens or shortens. The highest isometric force level is P_o (different to the P_o in the Hill equation) and is achieved at the optimal length for force production, L_o. The force length relationship is illustrated in Figure 2.7.

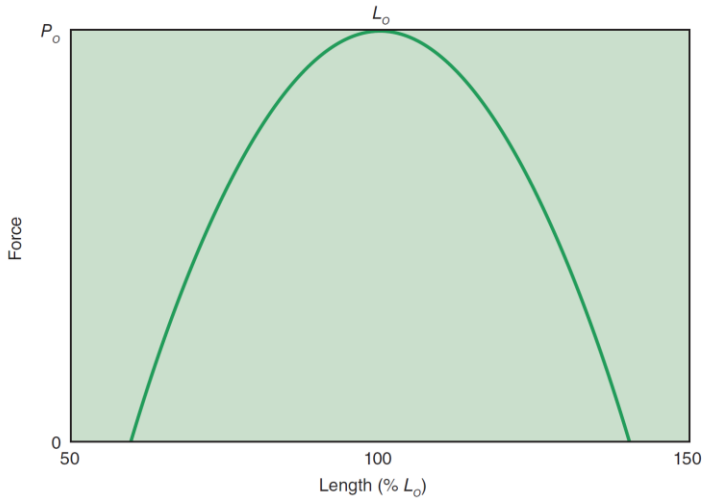

Figure 2.7: The force length relationship [32]

When a force is required, the CNS sends a nervous signal to the muscle in the form of stimulation. This causes an activation according to the SA relationship. The level of activation is controlled by the CNS according to the amount of force required. This control is exerted by changing the kinematic state of the CC that results from the FV and FL relationships.

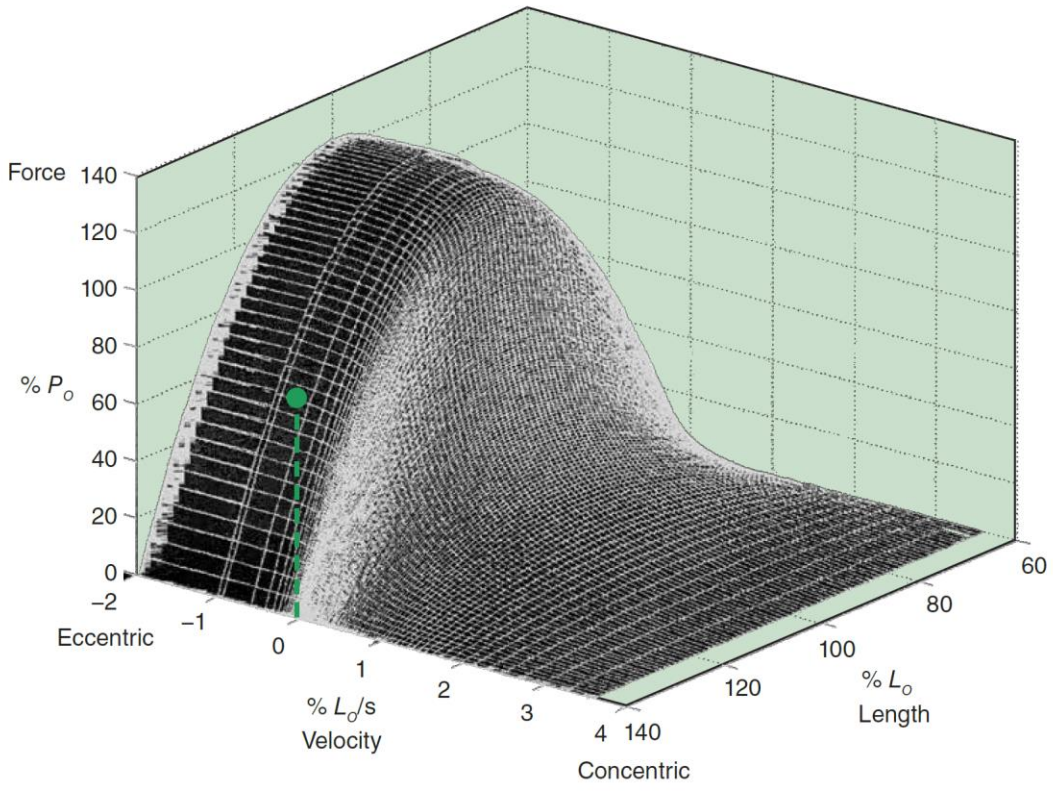

Figure 2.8: Force, velocity, and length relationship [32]

2.7.2.2 Series Elastic Component (SEC)

The SEC represents the elastic materials within and related to the muscle that are related to the passive connective tissue. This includes the tendons, aponeurosis, and connective elements within the muscle fibers. Any force produced by the CC is also expressed along the SEC [32].

2.7.2.3 Parallel Elastic Component (PEC)

PEC refers to the elastic response of an inactive muscle due to an external force. It represents structures like the fascia. It can also play a role during active force production [32].

2.7.3 Muscle Architecture

Muscle architecture refers to the anatomical characteristics that influence the mechanical properties of the Hill muscle model.

The pennation angle, which is the orientation of the muscle fibers with respect to their tendon, greatly affects the force production of that muscle. Fibers running parallel to the tendon would produce a greater force in that direction then fibers at an angle to the tendon where the same amount of force would be divided into x and y components.

Pennate muscles have shorter fiber lengths than fusiform muscles and can therefore produce a high amount of force.

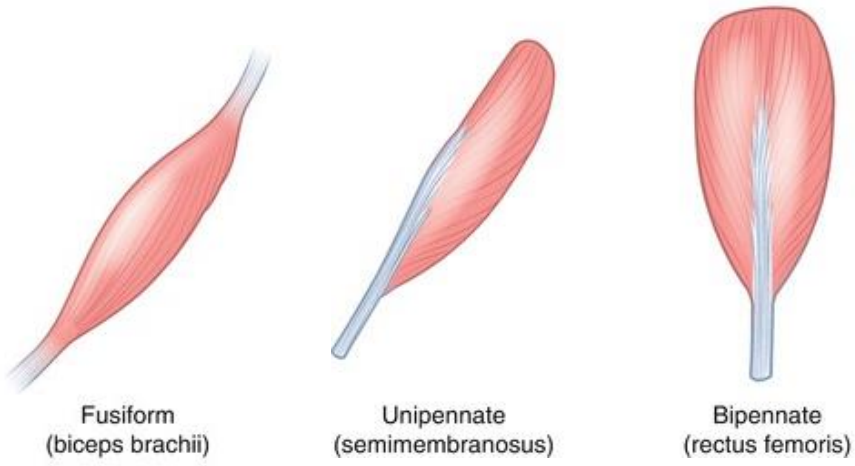

Figure 2.9: Different muscle architectures [34]

The muscles' cross-sectional area (CSA), and thus its force producing capacity, is defined by the number of sarcomeres connected in parallel. Since the CSA, the fiber

lengths, and the fiber orientation varies along the muscle length, the physiological cross-sectional area (PCSA) is used to as an estimate of a muscle's force.

$$PCSA = \frac{Muscle\ Volume}{Fiber\ Length} \tag{2.2}$$

The muscle-tendon unit is unique for each muscle and determines the amount of force it produces. The FL and FV characteristics depend on the length and thickness of the tendon as well as the number of sarcomeres in series in the specific muscle. The more sarcomeres there are in series, the greater the elasticity of the muscle. A long tendon would allow for smaller changes in muscle fiber lengths for a given movement. This enables it to operate at lower fiber velocities producing a given force at lower activation levels.

2.8 Techniques used for Gait Analysis

Motion capture systems are used to collect kinematic data from a moving subject. Markers are placed on key positions on the body of the subject and the coordinates of the markers are recorded. Multiple cameras are used to ensure that 3D coordinates are recorded without missing any marker.

Typical sensors used in biomechanics include inertial sensors comprising accelerometers, gyroscopes, and sometimes magnetometers; electromagnetic sensors; linear sensors; and array sensors. There are multiple tools used to measure force and moments of force for kinetic calculations. These include force platforms, force transducers and pressure distribution sensors. Internal forces from individual ligaments, tendons and joints cannot be measured without invasive procedures. Muscle strength capabilities can be measured using dynamometers which measure the torque of a subject at a single joint inder controlled kinematic conditions such as isometric, isotonic, or isovelocity [32].

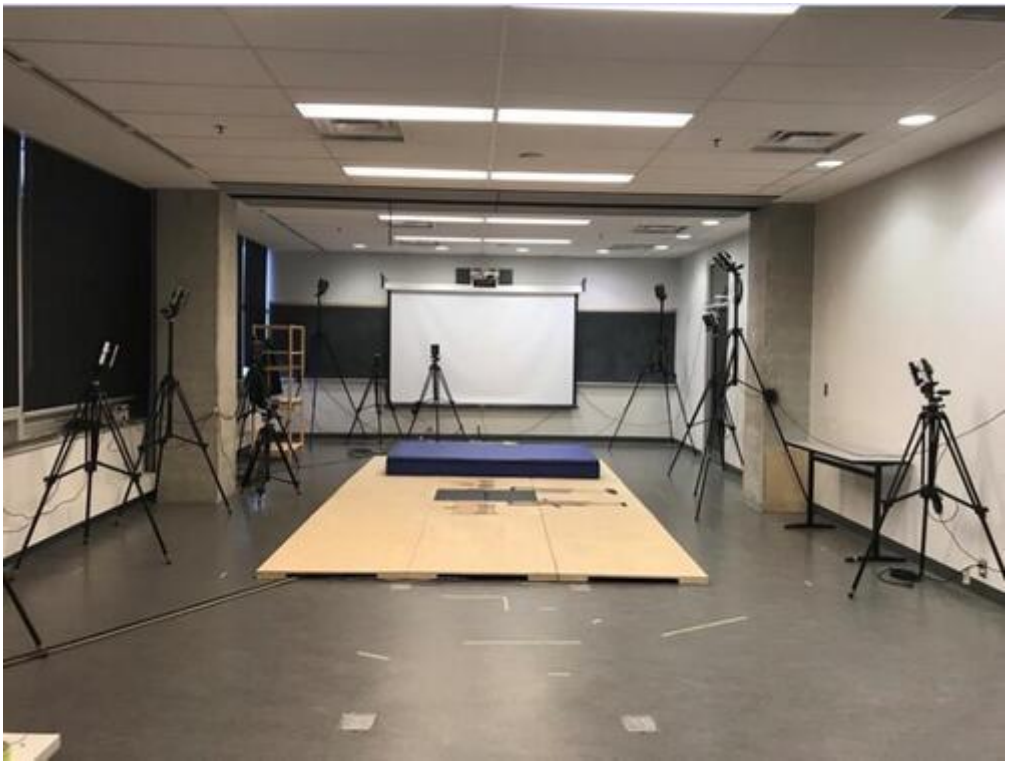

Figure 2.10: Motion Capture Lab, Univerity of Waterloo [35]

These kinematic and kinetic measurements are then digitized and processed using a computer where they are synced with musculoskeletal models. These are then used to perform modelling studies such as this one.

Some of the commonly used marker-based optoelectronic motion capture devices include Vicon, Qualisys, OptiTrack, and Motion Analysis. Topley and Richards [36] compared the different models available from these enterprises. The comparisons are presented in tables Table 2.1, Table 2.2, Table 2.3

A Quantum FaroArm is a preeminent portable coordinate measuring machine (PCMM) that allows manufacturers easy verification of product quality by performing 3D inspections, tool certifications, CAD comparison, dimensional analysis, reverse engineering, and more.

Table 2.1: Distance measurement errors for the top two rotating arm markers [36]

System	Difference (mm)	Standard Deviation	Max Error
Vicon, 16MP	0.539	0.058	0.675
Qualisys, 12MP	0.200	0.098	0.449
OptiTrack, 4.1MP	-0.283	0.005	0.417
Motion Analysis, 4MP	-0.585	0.103	0.815
Vicon, 4MP	0.486	0.109	0.822
Qualisys, 4MP	0.205	0.075	0.403
Qualisys, 2MP	-0.320	0.063	0.534
OptiTrack, 1.7MP	-0.219	0.070	0.450
OptiTrack, 1.3MP	-0.259	0.079	0.496
Motion Analysis, 1.3MP	-0.435	0.213	1.030

Difference is the average calculated system measurement compared to the FaroArm calculated marker distance

Table 2.2: Distance measurement errors for the top two plate markers [36]

System	Difference (mm)	Standard Deviation	Max Error
Vicon, 16MP	0.080	0.092	0.440
Qualisys, 12MP	0.085	0.116	0.537
OptiTrack, 4.1MP	-0.036	0.053	0.182
Motion Analysis, 4MP	-0.069	0.093	0.505
Vicon, 4MP	0.126	0.100	0.523
Qualisys, 4MP	0.034	0.095	0.308
Qualisys, 2MP	-0.035	0.213	0.722
OptiTrack, 1.7MP	-0.033	0.096	0.315
OptiTrack, 1.3MP	-0.259	0.084	0.266
Motion Analysis, 1.3MP	-0.003	0.232	0.991

Difference is the average calculated system measurement compared to the FaroArm calculated marker distance

Table 2.3: Calculated angle measurement errors [36]

System	Difference (mm)	Standard Deviation	Max Error
Vicon, 16MP	-0.203	0.085	0.284
Qualisys, 12MP	-0.235	0.121	0.657
OptiTrack, 4.1MP	-0.187	0.052	0.348
Motion Analysis, 4MP	-0.206	0.141	0.772
Vicon, 4MP	-0.196	0.136	0.856
Qualisys, 4MP	-0.130	0.104	0.492
Qualisys, 2MP	-0.148	0.168	0.850
OptiTrack, 1.7MP	-0.165	0.101	0.559
OptiTrack, 1.3MP	-0.148	0.101	0.472
Motion Analysis, 1.3MP	-0.012	0.483	2.083

Difference is the average calculated system measurement compared to the FaroArm calculated angle

Other systems are also available on the market which include Virdyn Full Body Function Inertia Motion Capture Suit and SMART DX EVO. With present day technological advances, markerless motion capture is making a breakthrough. Theia Markerless Inc. is a Canadian company whose markerless motion capture was the first ever markerless system validated as accurate as marker-based systems. Markerless systems allow for a simpler, faster, and more comfortable set up which enables more accurate data.

2.9 Musculoskeletal Models in Literature

Raabe and Chaudhari [37] developed and validated a full body OpenSim Model with a higher physiologically accuracy. Built upon three previously developed models, it is made up of 21 segments and has 30 degrees of freedom and 324 musculotendon actuators. The model is useful for detailed lower back modelling as each lumbar vertebra is modelled as an individual body and coupled constraints are implemented to

describe the net motion of the spine. Moreover, eight major spinal groups are modelled with multiple fascicles which allows forces to act in multiple direction. The model is validated and made freely available on the SIMTK website.

A detailed lumbar spine and lower limb model was developed by Favier et al. [38] which was then assessed against in vivo measurements for a range of spinal movements representing daily life activities. It was also validated against electromyographic studies with acceptable results.

Marjolein et al. [39] used a previously existing model developed by Delp et al. [40] to determine robustness of human gait against muscle weakness. Each of the leg muscles was atrophied in succession and predictive simulation was performed to determine the compensatory effect on other leg muscles. The muscle was then weakened in gradually until the model could no longer walk normally. This same process was also repeated by gradually decreasing the strength of all muscles simultaneously and studying the effects on the model's gait.

Ong et al. [41] also used the model by Delp [40] and the software, SCONE, to perform a predictive simulation of the effect of plantarflexor weakness and contracture on gait. An optimization framework was created and validated to generate realistic movements. They further used the model to study the speed as well as hip, knee and angle moments and flexion during a regular gait cycle.

CHAPTER 3

METHODOLOGY

Do people with lower back pain have dormant muscle function? This chapter lists the steps followed to establish whether the strength of the gluteus maximus has any effect on lower back pain by studying the effect of the forces in the lower back. We began our study using the software OpenSim but decided on using the software SCONE which is dedicatedly built for predictive modeling. We also carried out a study using a proprietary software, AnyBody Technology. These are presented below (Figure 3.1: Methodology.)

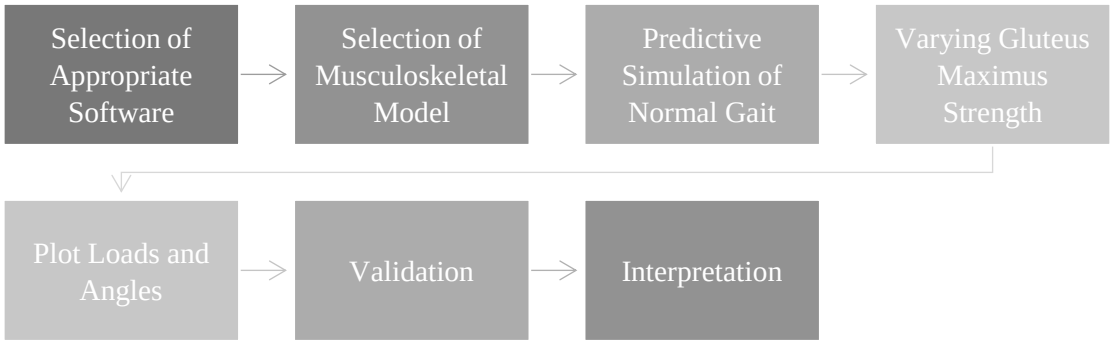

Figure 3.1: Methodology

3.1 Work Package 1 – OpenSim

OpenSim [42] is an opensource software for physics-based modelling of the movement and interaction of humans, animals, robots and the environment. It has the capability to allow users to build models from scratch containing rigid bodies, joints, muscles, as well as actuators, springs and dampers, constraints, contact and controllers. Since it is opensource, there is a large community contributing to an increasing number of musculoskeletal models, most of which can be accessed for free.

The Full Body Lumbar Spine (FBLS) model [37] (figure 3.1) was employed in OpenSim, version 3.3 to implement the study. This model was scaled according to the sample data. The subject was a 24-year-old male with a mass of 68.6 kg and a height of 1.7m.

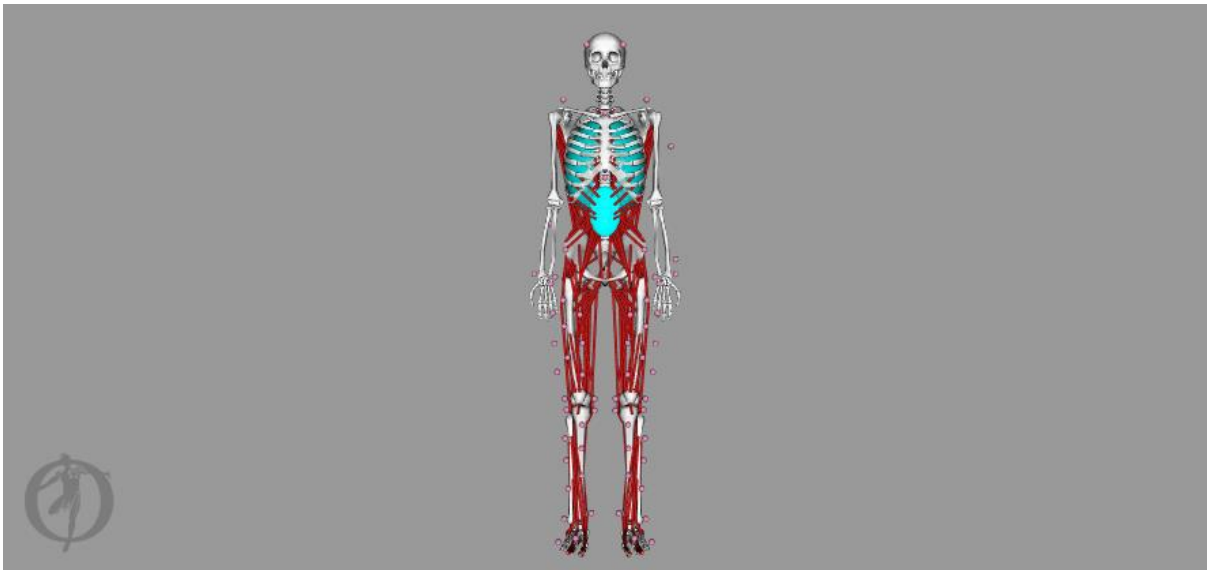

Figure 3.2: The Full Body Lumbar Spine (FBLS) model

Inverse Kinematics was used along with the sample marker data to compute the marker positions at each time step. The Residual Reduction Algorithm (RRA) was used to minimize the effects of modelling and marker data errors resulting in a model which is more consistent with the ground reaction force data. The control and kinematic results of RRA were used to run the forward dynamics tool in order to obtain the joint reaction forces on the lumbar vertebrae.

3.1.1 Test Cases undertaken as experimental approach:

A study was conducted at the biomechanics lab of Lahore University of Management Sciences (LUMS) to obtain kinematic files from a test subject. A male of 1.75 m weighing 62 kgs was instructed to move in a variety of patterns imitating everyday movements as well as movements used in weight training exercises. Markers placed on

the subject were tracked and recorded. However, due to technical failures in the C3D file, this data could not be processed further.

3.2 Work Package 2 – AnyBody Technology

AnyBody Technology [43] is a proprietary software dedicated for musculoskeletal modelling to investigate the mechanical functions of the human body. The software is able to estimate properties inside the body such as muscle and joint loads which are hazardous and difficult to obtain in vivo.

The accompanying AnyBody Managed Model Repository (AMMR) documentation contains a variety of ready-to-use models to work on. These include activities of daily living, ergonomics & exoskeletons, orthopedics and sports among others.

An existing example model of the cross-trainer model (figure 3.2) was used (with permissions from Anybody Tech Platform using a trial version) to perform the analysis. The cross-trainer model is most similar to a walking model. The model used is a male weighing 75 kg with a height of 1.75 m.

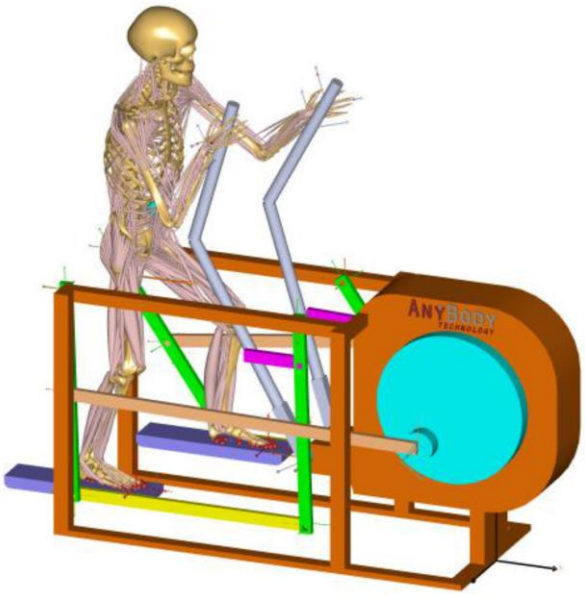

Figure 3.3: Cross Trainer Model

The strength of the muscles was varied by varying the strength index, which affected the physiological cross-sectional area (PCSA) factor of the muscle fibers. The PCSA factor determines the maximum force output at optimum fiber length of the muscle. In the AnyBody Modelling system, the PCSA factor is calculated using the following formula:

$$PCSA\ factor = Specific\ strength * Strength\ Index\ of\ the\ leg \quad (3.1)$$

here the specific strength is 90 N/cm^2 as is the default in the software.

A simple model of the muscles was used on the lumbar spine, which include the lumbar extensors and flexors, as the three-hill muscle model is computationally complex and requires finer controls. The lumbar discs were set to nonlinear stiffness and the lumbar ligaments were activated. Simple muscles were used in both the left and right legs. The strength indexes chosen were 1, 5, and 10, which are respectively the minimum, median, and maximum possible values. The analysis was run for only one second due to computational and time limitations.

For each strength index, the proximodistal joint reaction forces at the interface of each lumbar vertebrae were computed using the simulation platform and plotted against gait cycle on the cross trainer. The proximodistal forces would be the forces on the y axis or the compressive forces acting on the sagittal plane. The interfaces of the simulation are as follows:

a. Sacrum-pelvis

b. L5-sacrus

c. L4-L5

d. L3-L4

e. L2-L3

f. L1-L2

3.3 Work Package 3 - SCONE

SCONE [44] is an opensource software dedicated for predictive modelling of the musculoskeletal system. It utilizes models along with an open loop or closed loop controller. Controllers produce input signals for the actuators of the model. An objective function describes the task for which the simulation is to be optimized. n Optimizer is to find the parameters for which an objective function is minimized or maximized, depending on the type of objective.

To implement the simulation, a gait model of a planar musculoskeletal (MSK) model of an adult of mass 75.16 kg and a height of 1.8 m was used [40]. The model can be found on the simtk repository and has been previously used to study the effect of plantarflexor weakness and contracture [41].

Figure 3.3 shows the model with nine DOF with a 3 DOF planar joint between the pelvis and the ground. The hip and ankles were represented using a single DOF pin joint while the knees were represented by a 1 DOF joint coupled with translation and rotation. Based on previous data, the lumbar joint was locked at 5˚ flexion [45]. Nine of the major leg muscles were represented by single muscle tendon units using the Hill muscle model [46]:

1. Gluteus maximus (GMAX)
2. Biarticular hamstrings (BFSH)
3. Iliopsoas (ILPSO)
4. Rectus femoris (RF)
5. Vasti (VAS)
6. Biceps femoris short head (BFSH)
7. Gastrocnemius (GAS)
8. Soleus (SOL)
9. Tibialis anterior (TA).

The peak isometric forces of the muscles were based on a previous musculoskeletal model whose muscle volumes were based on young, healthy adults [47, 48].

A predictive simulation software, SCONE [44], was used to train the model for a gait cycle of a maximum duration of 30 seconds and a minimum velocity of 0.5 m/s. Assuming all other variables are the same, the model was trained for a gluteus maximus strength ranging from 25 % - 150 % of the original maximum isometric force. These ranges would cover atrophy, normal strength, and hypertrophy of the GMAX muscles. The same initial position and velocities were given to each trial.

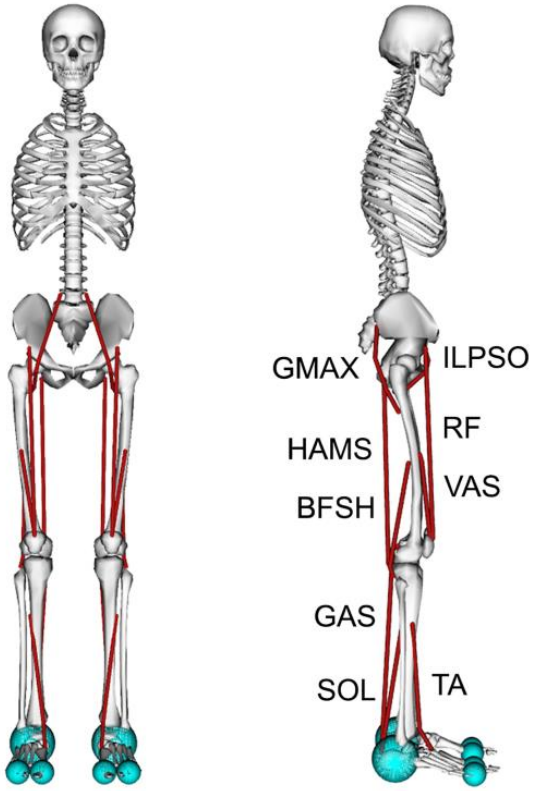

Figure 3.4: A planar musculoskeletal model for walking [41]

The model was trained till the best optimization score was reached. Optimization was based on the cost of transport, ensuring the model didn't fall and the ankle and knees didn't hyperextend or hyperflex outside of natural limits. These measures ensure the gait pattern doesn't take on abnormal patterns.Equation 4 shows the objective function. Further details about the model can be found in the article by Ong et al. [41].

$$J = w_{cot}J_{cot} + w_{spd}J_{spd} + w_{inj}J_{inj} + w_{head}J_{head} \qquad (2)$$

where the goal is to

- Minimize J_{cot} the gross cost of transport
- Maintain J_{spd}, average speed over each avoiding falling
- Avoid ligament injury J_{inj}
- Stabilize the head J_{head}

The optimized models were then used to analyse the results. The back, hip and knee loads were plotted and analysed against the gait cycle for GMAX max isometric forces of 25% the normal, 100% of the normal and 150% of the normal with the normal GMAX max isometric force being 1944N. The loads are normalized by the body weight where,

$$load = joint\_force \,/\, (\, model\_mass * g \,) \tag{3.3}$$

with g being gravity, i.e, 9.80665 m/s^2.

The models were simulated on a 64-bit operating system with an Intel(R) Core(TM) i7-3770 CPU, an NVIDIA GeForce GTX 750 Ti graphics card and Windows 10 with 8 GB of RAM running at 3.40GHz. On this system, the thirty second simulations took anywhere from 10 – 12 hours to optimize.

The pelvic tilt and hip and knee angles are measured in radians and plotted against the gait cycle. The forces produced by the GMAX and the hamstrings were also examined to find how the strength and PCSA of GMAX affects the need for force production by each of these muscles.

The back load was measured at the joint between the sacrum and the lowest lumbar vertebrae. The hip load was measured from between the pelvic bones and femur and the knee load was measured at the joint between the femur and tibia. This is illustrated in figures 3.4 and 3.5. Figures 3.6 – 3.8 illustrate the pelvic tilt and the hip and knee flexions and extensions. The results obtained from these work packages are described in the next section.

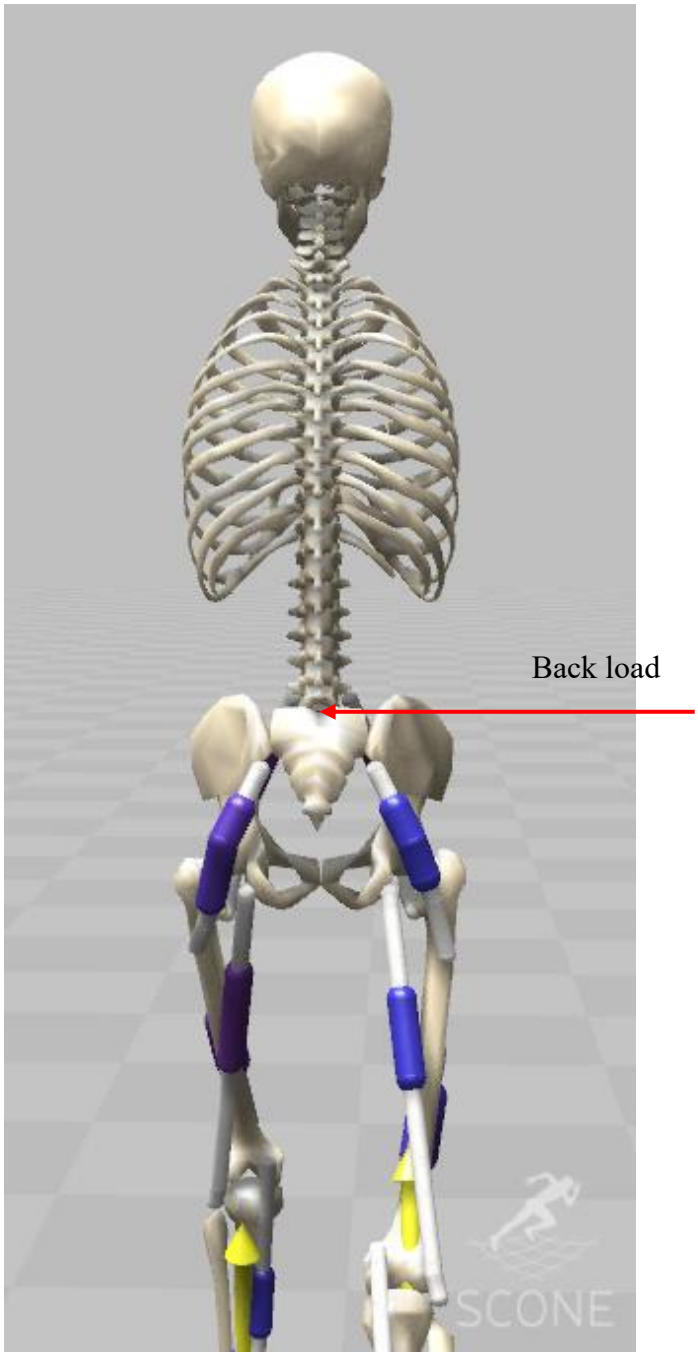

Figure 3.5: Position between S1 and L5 where back load is calculated

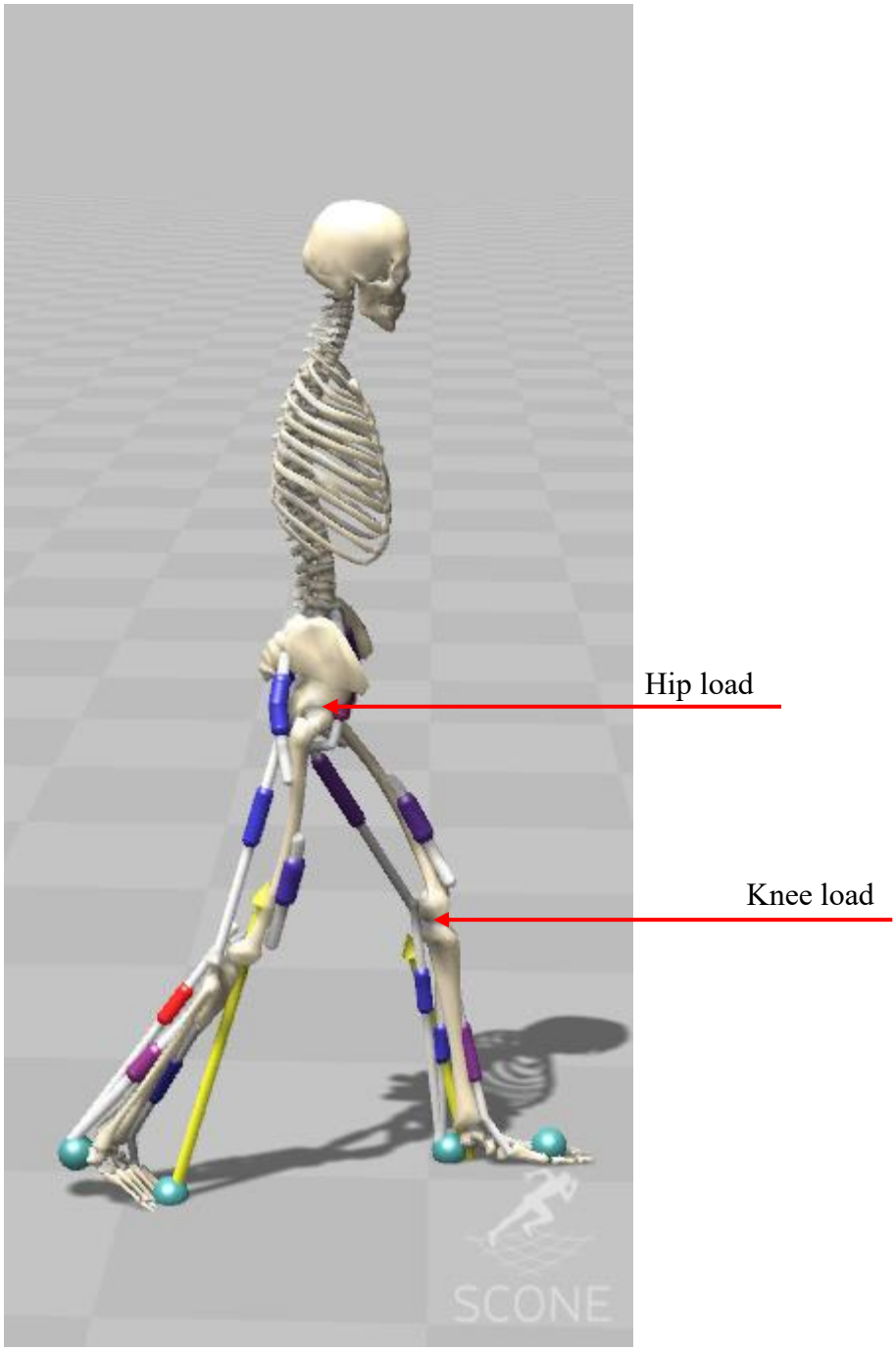

Figure 3.6: Hip load computed between the pelvis and femur. Knee load computed between the femur and the tibia

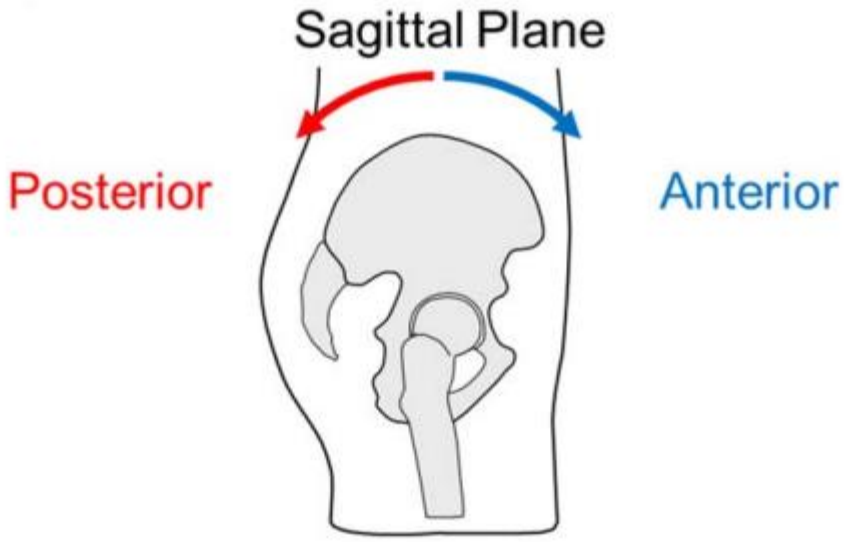

Figure 3.7: Pelvic tilt [49]

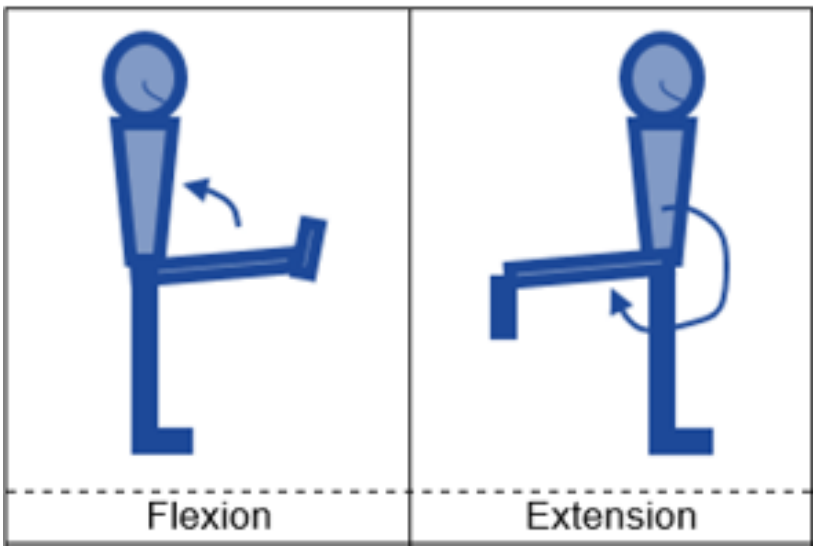

Figure 3.8: Hip flexion and extension [50]

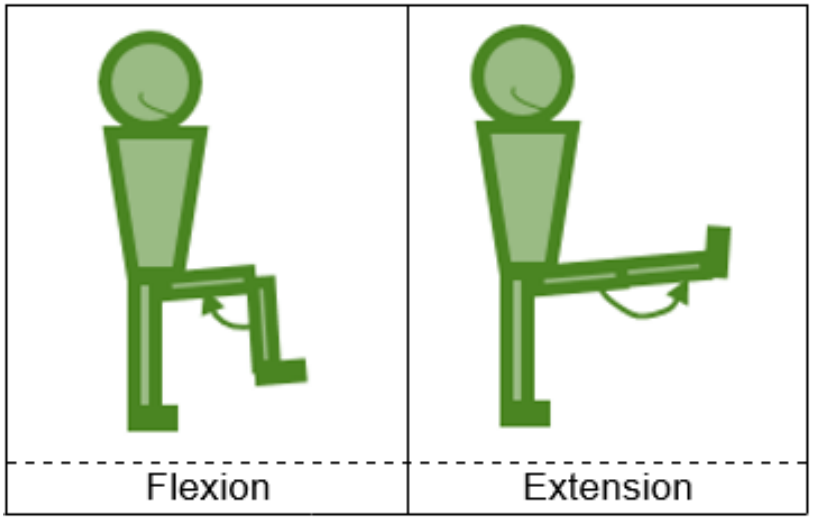

Figure 3.9: Knee flexion and extension [50]

Biomechanical gait impairments in individuals with LBP may be captured by changes in spatiotemporal characteristics. These properties can include speed or step length, kinematic characteristics such as joint/segmental motion or coordination between joints/segments, and kinetic characteristics like forces and torques, and electromyography (EMG) characteristics like amplitude or timing of muscle activation.

The amount of trunk motion and joint loading during gait is relatively low compared to other activities such as climbing stairs and lifting weighted object. These studies can be further explored using the current model respectively.

CHAPTER 4

RESULTS

4.1 Work Package 1 – OpenSim

The utility of Opensim has already been explained in section 3.1. In this work package pelvic tilt, flexion and extension of knee and hip is computed. There is a need to understand that any loads and motions exerted on the human body can cause instability in the lumbar spine. The state of spinal instability can thus lead to injury/damage. Pelvic tilt, hip & knee movement can be used as a key parameter to understand strains encountered on lumbar spine.

The plots in Figure 4.1 to Figure 4.6 show time on the x axis, and the angle in radians on the y axis. Negative values on the pelvic tilt indicate an anterior tilt and vice versa. The hip and knee angles indicate extension as positive and flexion as negative on the y axis with 0 indicating a completely straight knee and/or hip.

It can be seen that the plotted lines are noisy for the result of inverse kinematics, and they smooth out after reducing the residuals. This shows the importance of the residual reduction algorithm.

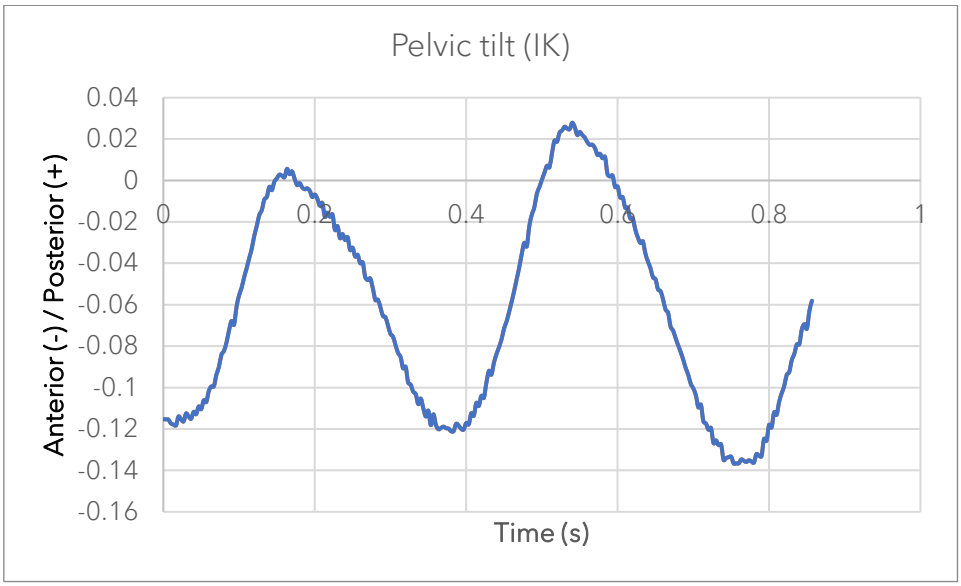

Figure 4.1: Pelvic tilt for inverse kinematics shown in radians

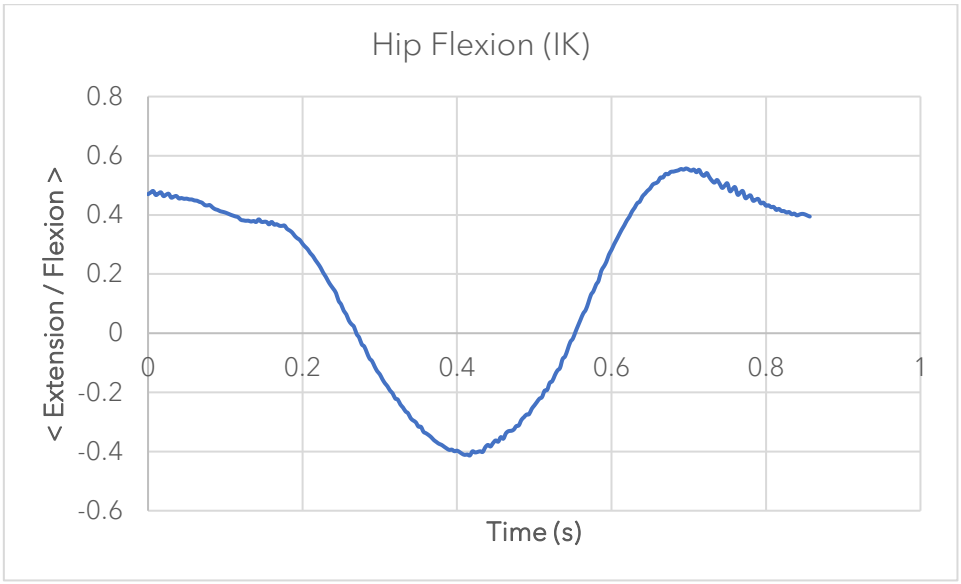

Figure 4.2 : Hip flexion for inverse kinematics shown in radians

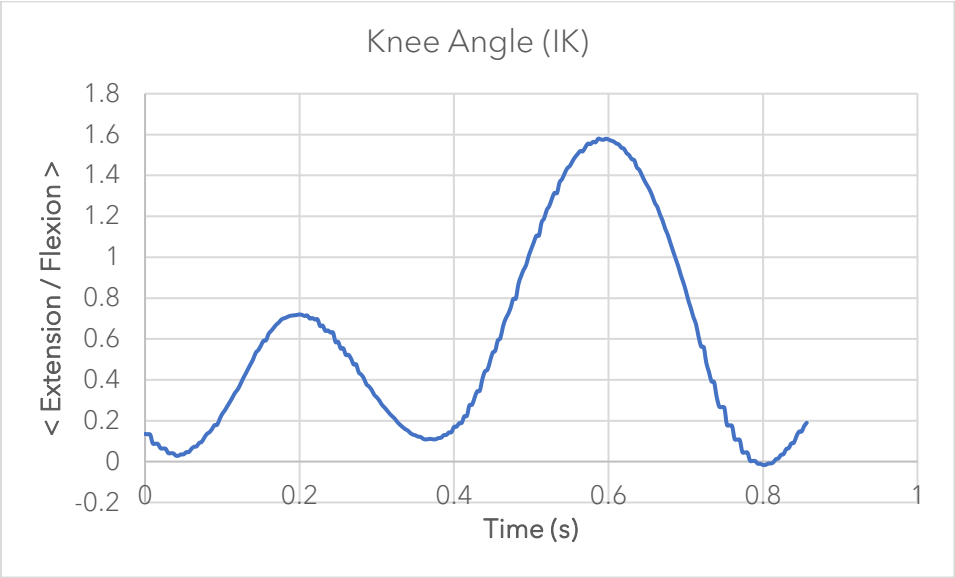

Figure 4.3: Knee angle for inverse kinematics shown in radians

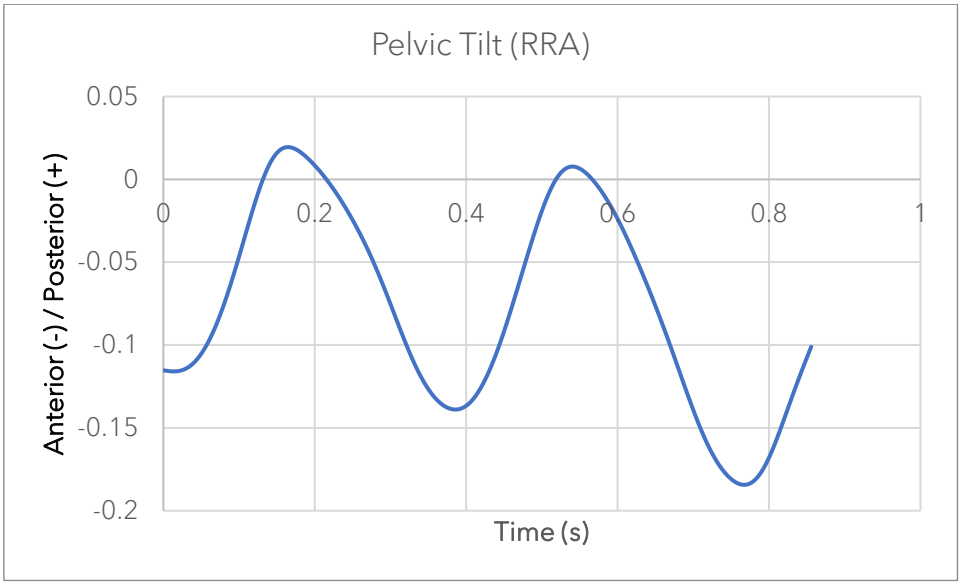

Figure 4.4: Pelvic tilt for residual reduction algorithm shown in radians

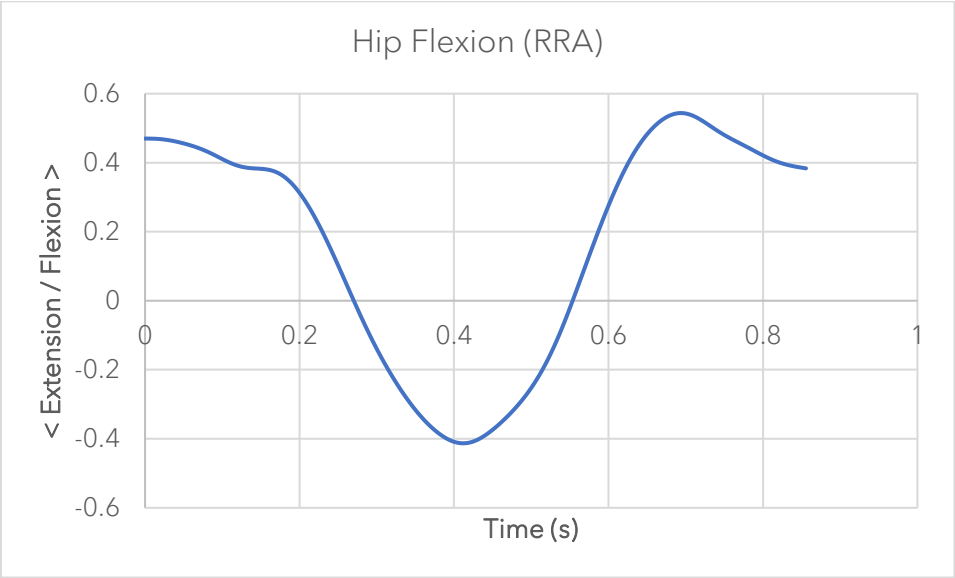

Figure 4.5: Hip flexion for residual reduction algorithm shown in radians

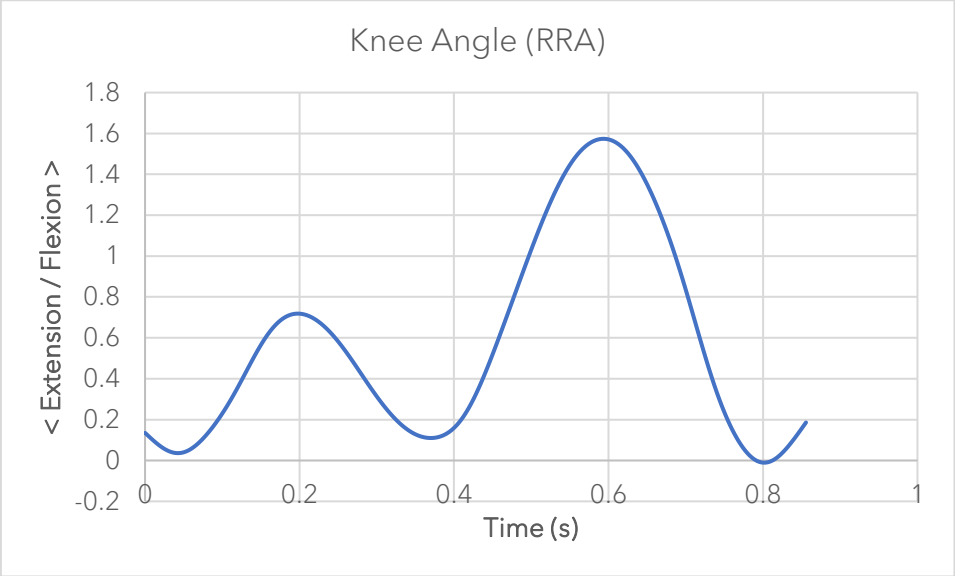

Figure 4.6: Knee angle for residual reduction algorithm shown in radians

In order to compute the effect of the change in GMAX muscle forces on the lumbar joints, forward dynamics simulation had to be performed. But due to the complexity of the model, the model “crumpled” up and failed to run properly. This is illustrated in .Figure 4.7.

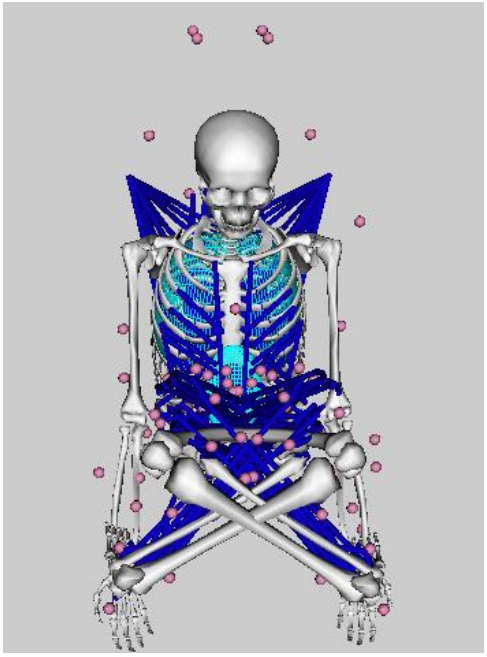

Figure 4.7: Crumpled up model after running the forward dynamics simulation

Therefore, it is recommended to carefully handle model complexity, inaccuracies in geometry or load distribution may cause model to fall. The perturbation caused in the model geometry due to any of these can result in unexpected motion or behaviour as shown in figure 4.7.

4.2 Work Package 2 – AnyBody Technology

Using Anybody Technology delivered a fine solution to calculating loads on the vertebrae. For example, the plots from figures Figure 4.8 to Figure 4.13 show the load on to each of the vertebrae from L1 to the sacrum-pelvis joint. The gait cycle is on the x axis, and joint reaction forces normalized by body weight are on the y axis.

The results show that the overall proximodistal joint reaction force at each interface is the most at the minimum muscle strength index of 1. As the strength index is increased to 5, the overall joint reaction forces decrease. However, no significant change is observed between the JRF at the strength index of 5 and the strength index of the maximum possible value of 10.

To ensure that the resultant values are valid, they were compared against a the work of Favier et al. where they quantified the intersegmental spine joint reaction forces during everyday activities [38]. The range of the JRFs are similar and therefore the results can be considered valid.

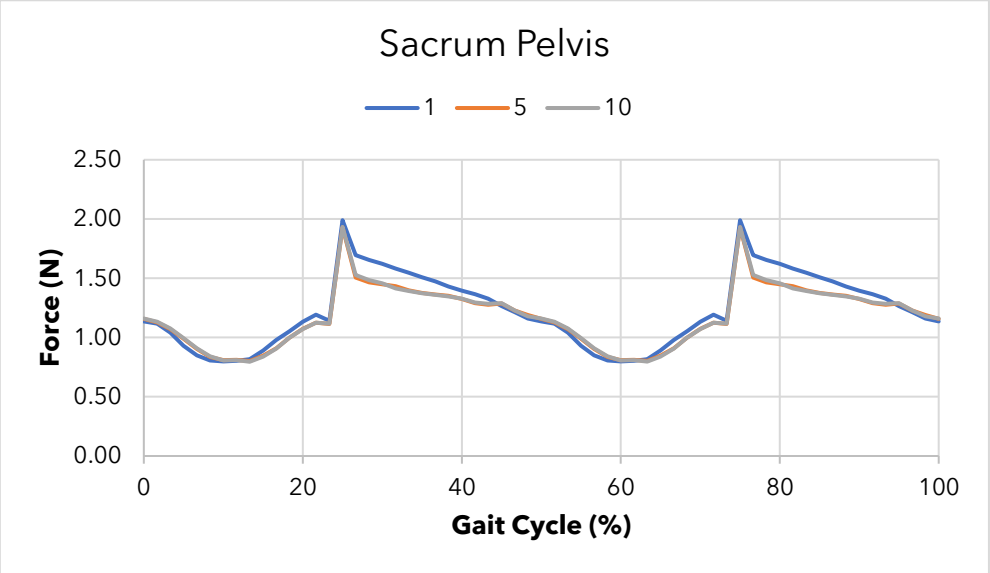

Figure 4.8 The load of the sacrum onto the pelvis as computed by Anybody technology. 1, 5, and 10 represent the strength indexes.

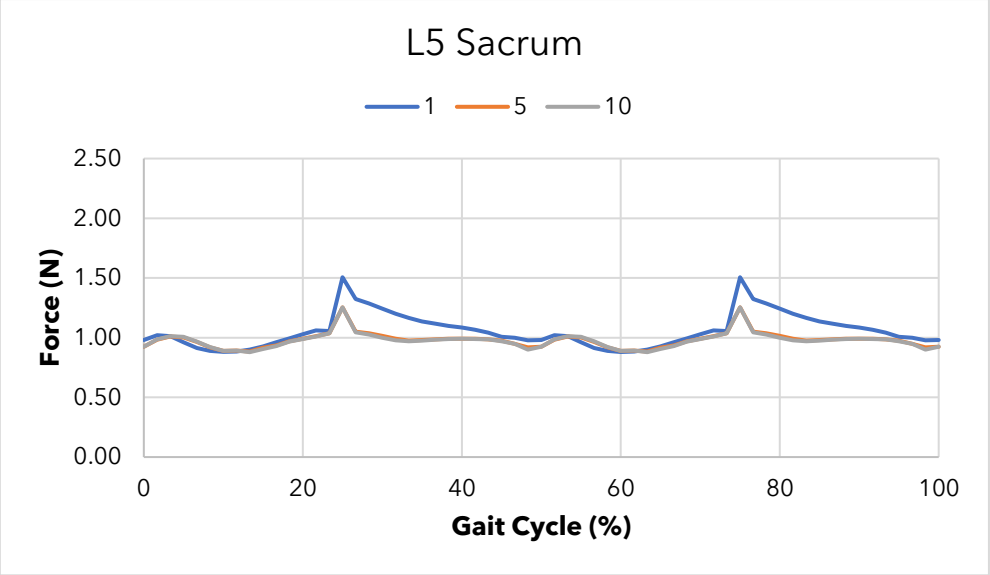

Figure 4.9: The load of the L5 onto the sacrum as computed by Anybody technology. 1, 5, and 10 represent the strength indexes.

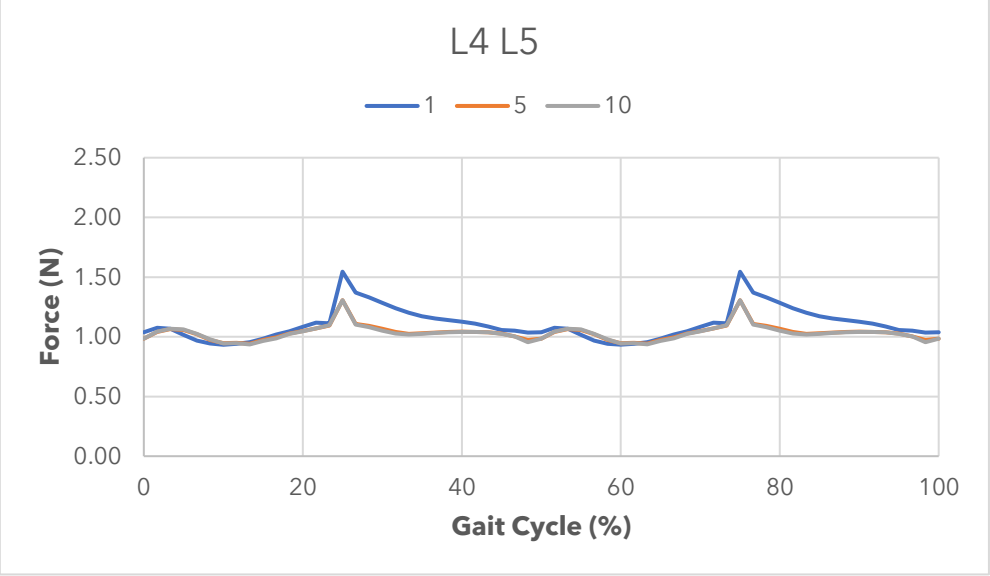

Figure 4.10: The load of the L4 onto the L5 as computed by Anybody technology. 1, 5, and 10 represent the strength indexes.

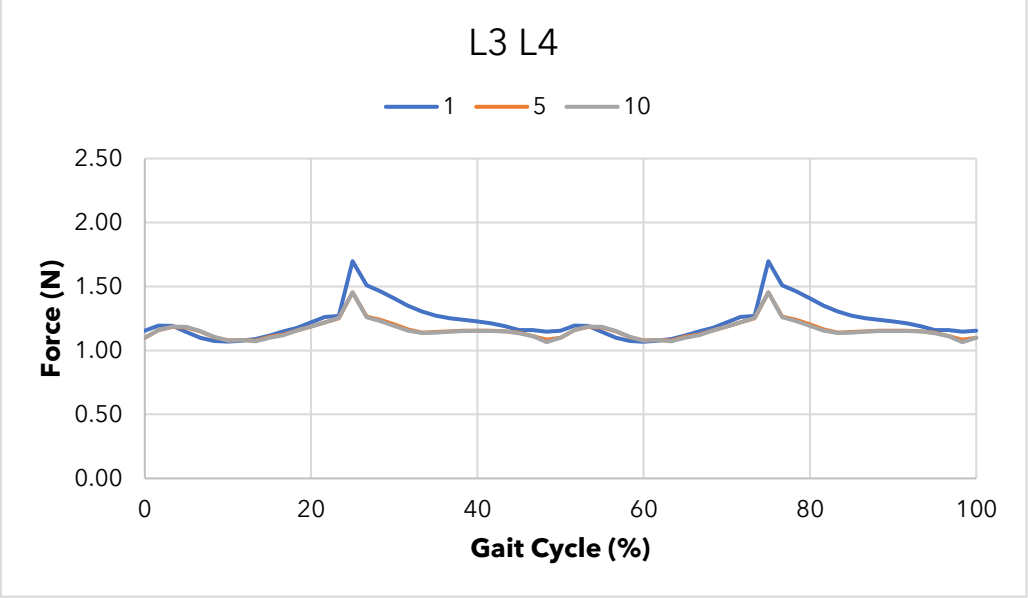

Figure 4.11: The load of the L3 onto the L4 as computed by Anybody technology. 1, 5, and 10 represent the strength indexes.

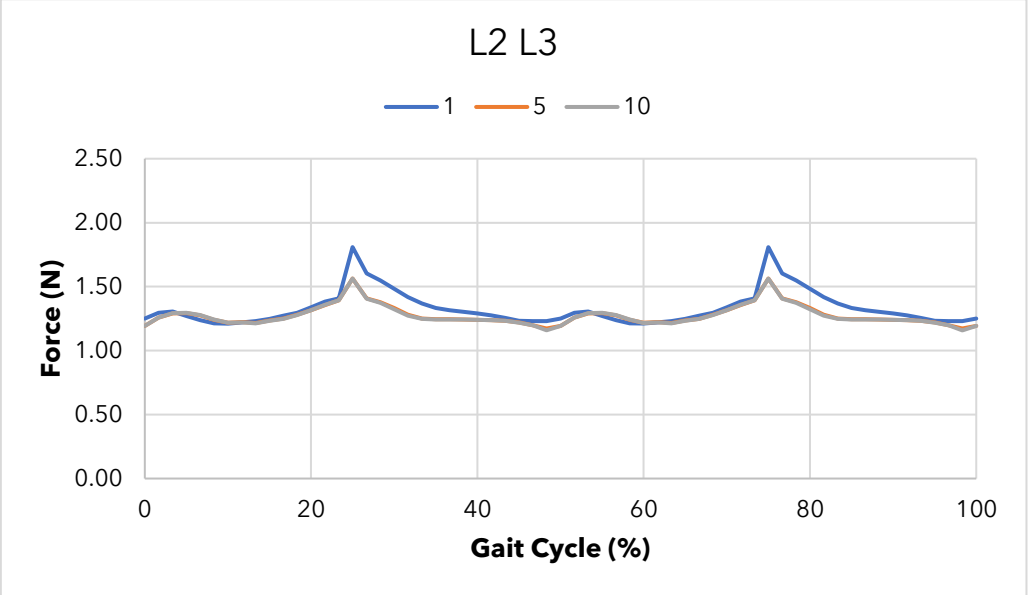

Figure 4.12: The load of the L2 onto the L3 as computed by Anybody technology. 1, 5, and 10 represent the strength indexes.

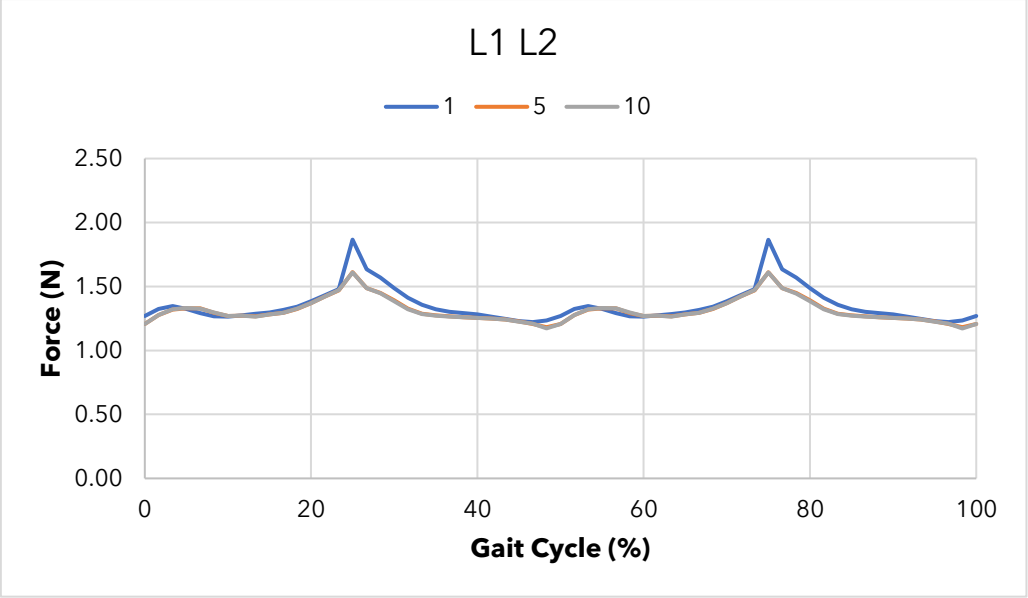

Figure 4.13: The load of the L1 onto the L2 as computed by Anybody technology. 1, 5, and 10 represent the strength indexes.

The JRF varies as the model moves since the acceleration of each vertebrae varies according to its co-ordinates at each time step. As the strength of the leg muscles is increased, lower inter-segmental spine joint reaction forces are observed. This indicates lower compressive forces and lower stresses on the intervertebral discs. Increasing the strength of the leg muscles decreases the inter-segmental spine joint reaction forces to a certain limit after which any further increase in strength causes a negligible decrease in the JRF.

This we were able to publish as a book chapter, to understand the significance of muscle in lower back mechanics [51].

4.3 Work Package 3 – SCONE

The ultimate objective of using SCONE was to utilize a validated models across the wide range of muscle indices. In comparison to the OpenSim our model prematurely

failed due to the limitations/constraints mentioned in section 4.2. Therefore, SCONE was utilized as a mature resource for this particular study.

Figure 4.14 illustrates the gait cycle with the right heel striking at the initiation of the cycle at 0% which then leads to left toe lifting off the ground. This is followed by foot flat as the left leg swings forward and finally the left heel strikes the ground at 50% of the gait cycle. The process is repeated as the right foot lifts off the ground and goes into swing phase ending with the right heel striking the ground. This completes a single gait cycle, and the process is repeated for the next gait cycle.

While walking, the model with atrophied GMAX exhibited a high amount of movement of the spine in the sagittal plane. With each step, the model leaned back and tilted forward in an exaggerated manner. On the contrary, the model with hypertrophied GMAX exhibited a more upright, stable posture during the entire gait cycle.

Dynamic instability of the spine would lead to an increased rate of wear and tear. Over time, this could manifest in the form of crippling disorders such as disc herniation and nerve damage which are some major causes of chronic lower back pain.

Figure 4.15 to Figure 4.24 illustrate the variations in back, hip, and knee loads as well as the pelvic tilt, hip flexion and knee angle across the gait cycles. Each of the variables are plotted for three muscle strengths where 0.25 represents an atrophied gluteus maximus with a maximum isometric force of 486N, 1.0 represents the unaltered model with a maximum isometric force of 1944N, and 1.5 represents a hypertrophied gluteus maximus with a maximum isometric force of 2916N.

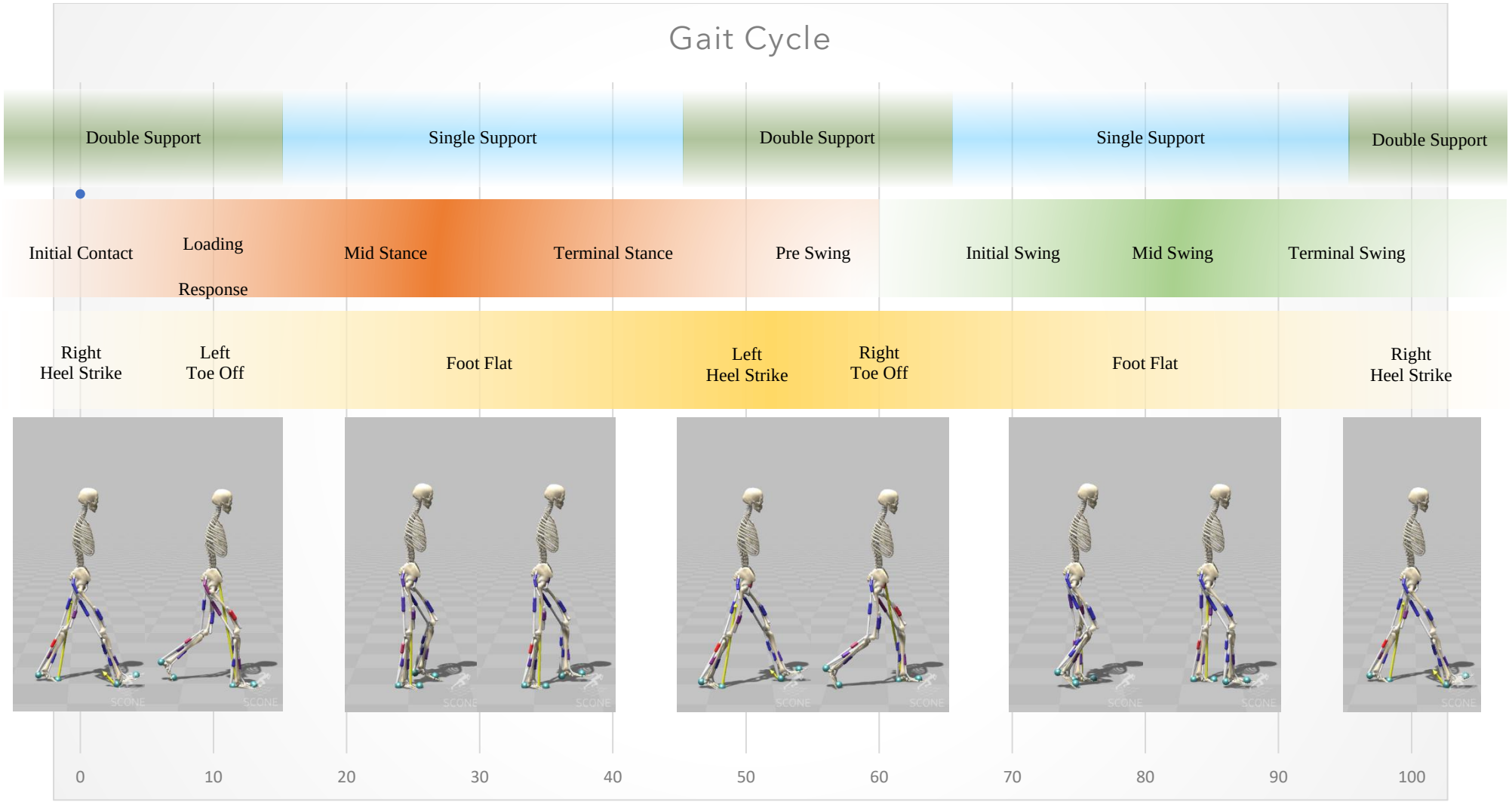

Figure 4.14: A single gait cycle of the model in SCONE

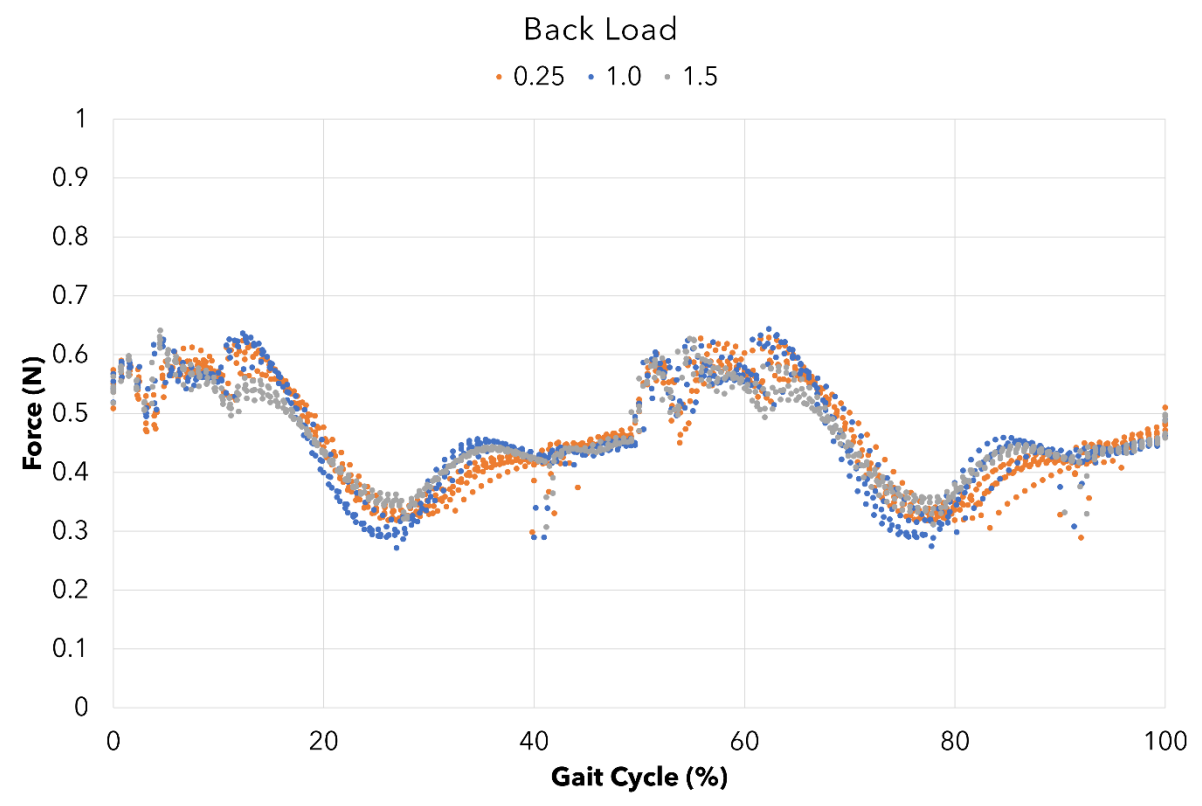

Figure 4.15: Back load, the load of L5 onto the sacrum, along a regular gait cycle as computed by SCONE.

The highest peaks are shown at 5 – 15 % and 55 – 65 % of the gait cycle signifying that the highest back load is between heel strike and toe off when both feet are the furthest apart. Valleys are shown at 25% and 75% during foot flat when both feet are closest together. Small peaks form at 35% and 85% when the swinging foot passes the body centre of mass and hip flexion begins. 35 – 50 % and 85 – 100 % show plateaus as the hip flexion continues before going up to a high peak signifying another heel strike.

The dystrophy of GMAX mostly affects the valleys when the feet are closest together showing an increase in compressive back loads during foot flat as compared to the unaltered model. The waveform is also slightly spread apart before the plateau.

In hypertrophy, the compressive forces still show an increase during the valleys, but they show a decrease in the peaks when the feet are furthest apart, i.e., at toe off, at 10%

and 60% of the gait cycle. This results in a lesser variation of loads during the entire gait cycle.

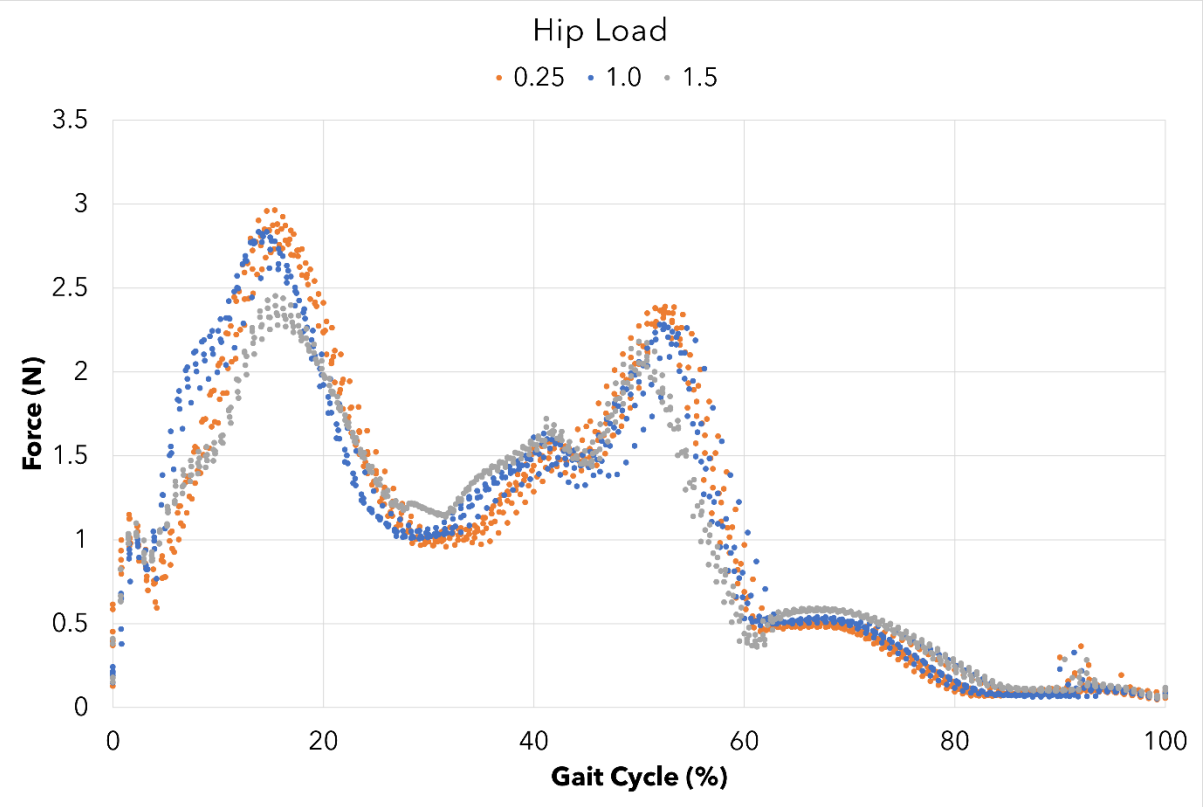

Figure 4.16: Hip load, the load of the pelvic bones onto the femur, along a regular gait cycle as computed by SCONE

The hip load shows its highest peak at 15% of the gait cycle when the contralateral foot toe lifts off. At 30%, a valley is formed when the foot is flat and both feet get closer together before passing each other. From 30 – 50% of the gait cycle, the load increases and reaches another peak as the contralateral heel strikes the ground. A sharp decrease in the load is shown as the ipsilateral toe lifts off, and most of the load shifts to the contralateral hip. Finally, the load shows a steady decline as this foot moves into the swing phase.

Atrophy of the GMAX shows an increase in the hip loads during the peaks as compared to the unaltered model. The valleys are at a similar load for both the atrophied and unaltered model; however, it is slightly shifted to the right and spread out for a longer

period of the gait cycle in atrophy. In hypertrophy, the hip loads show a considerable decrease in the high peaks indicating a lower hip load with a stronger GMAX. The valley, however, shows a slight increase in compressive hip load with an increase in GMAX strength. The overall variability of the hip load is lesser than with an unaltered GMAX strength.

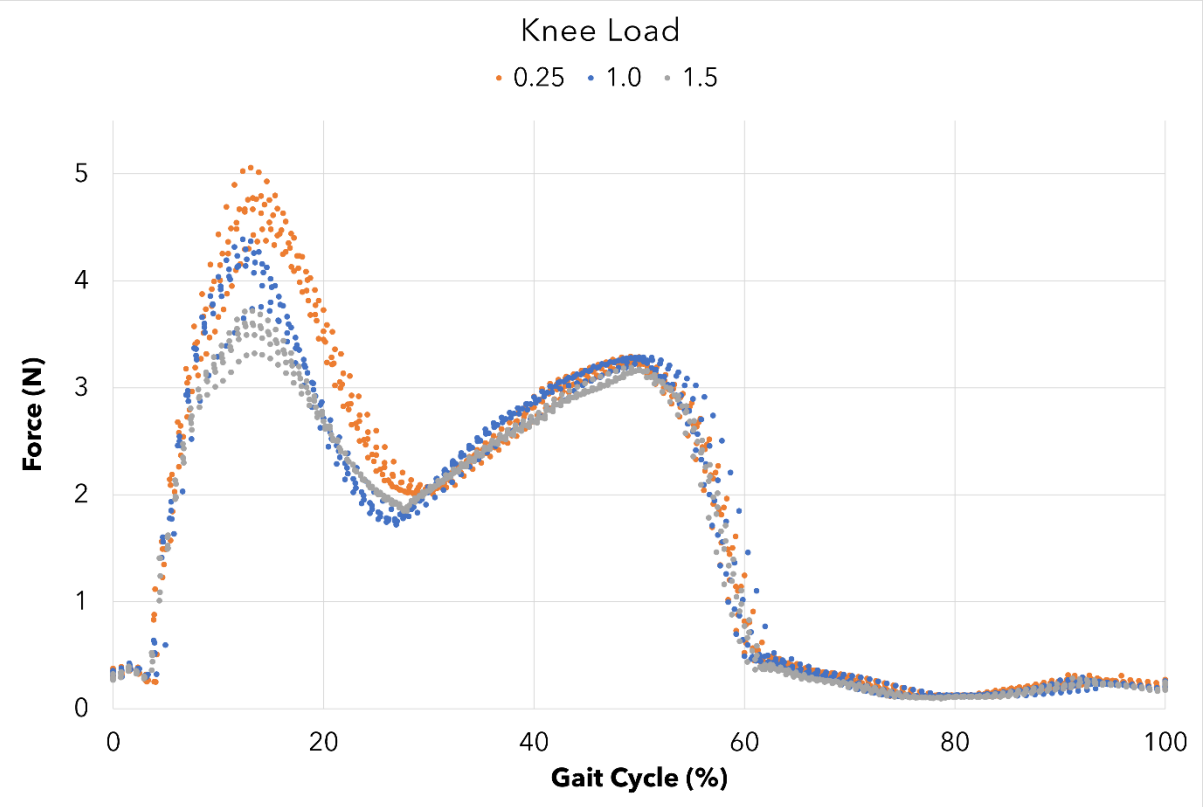

Figure 4.17: Knee load, the load of the femur onto the tibia, along a regular gait cycle as computed by SCONE

A high knee load is observed right after the contralateral toe lifts off the ground and the weight shifts to the ipsilateral leg. As the feet grow closer together, the load decreases and begins to increase again as the feet pass each other. At 50% of the gait cycle, when the contralateral heel strikes, the load shows another peak before a sharp drop as the ipsilateral toe lifts off.

A weaker GMAX results in higher knee loads from toe off of the contralateral foot to foot flat while a stronger GMAX results in lower knee loads during the same time. The remaining cycle show similar knee loads for all three GMAX strengths.

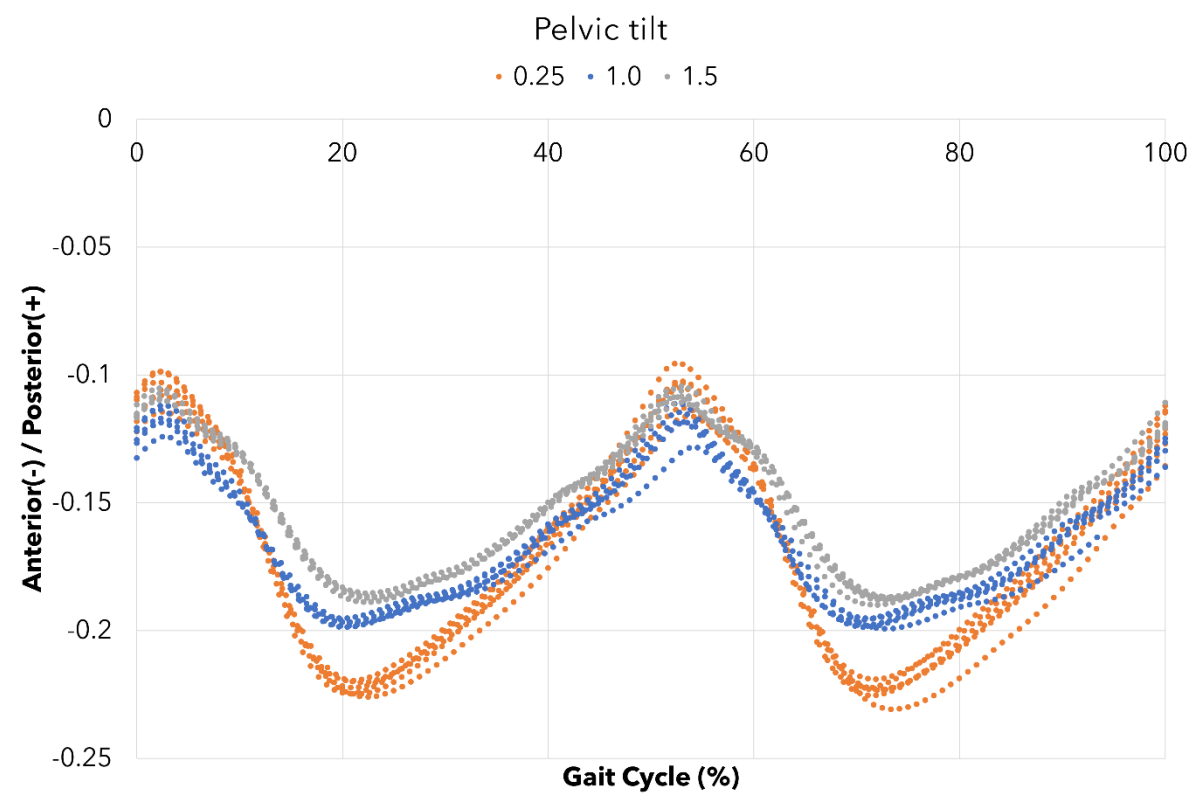

Figure 4.18: Pelvic tilt, the angle of the pelvis with the Z axis, along the gait cycle as computed by SCONE. Negative values represent anterior tilt and positive values represent posterior tilt.

The lowest pelvic tilt is shown at each heel strike when the feet are furthest apart. As the contralateral toe lifts off and passes the centre point, the anterior pelvic tilt reaches its highest value before decreasing to its original value as the contralateral heel strikes the ground and the cycle repeats.

As the GMAX weakens, there is a remarkable increase in the anterior pelvic tilt during foot flat. However, during heel strike at 0 and 50% of the gait cycle, the anterior pelvic tilt is lesser than that with an unaltered GMAX strength. This results in a larger range of motion in the atrophied model causing an unstable gait.

With a stronger GMAX, the entire gait cycle shows a decrease in the anterior pelvic tilt indicating a more stable pelvis and back.

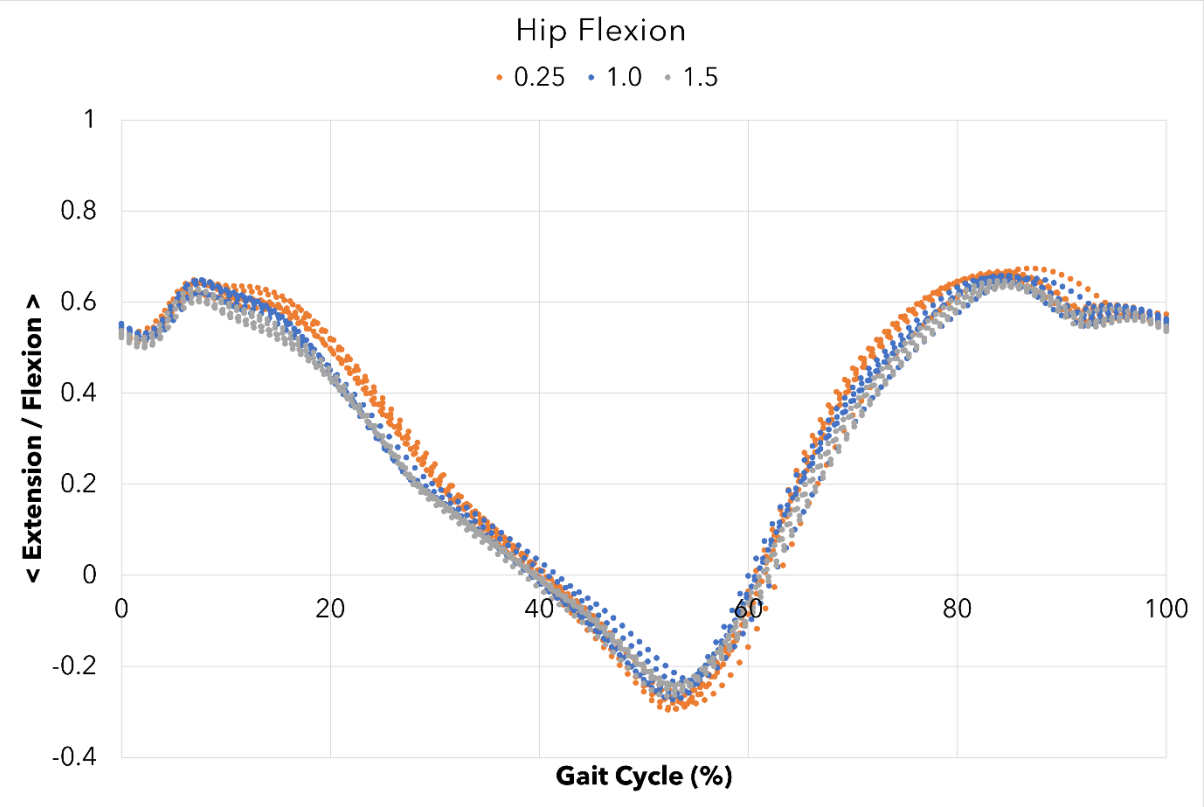

Figure 4.19: Hip flexion along the gait cycle as computed by SCONE. Negative values represent extension. Positive values represent flexion.

The maximal hip flexion occurs as the contralateral toe lifts off the ground and decreases steadily as the ipsilateral hip extends. After the contralateral heel strikes the ground, the ipsilateral hip is maximally extended. The hip begins to flex again as ipsilateral toe lifts off the ground and reaches another maximum slightly before the heel strike. A small dip occurs at heel strike and the same thing repeats for the next gait cycle.

The model shows a negligible difference in hip flexion with a change in gluteus maximus strength. The weaker GMAX shows a slight shift with respect to the gait cycle.

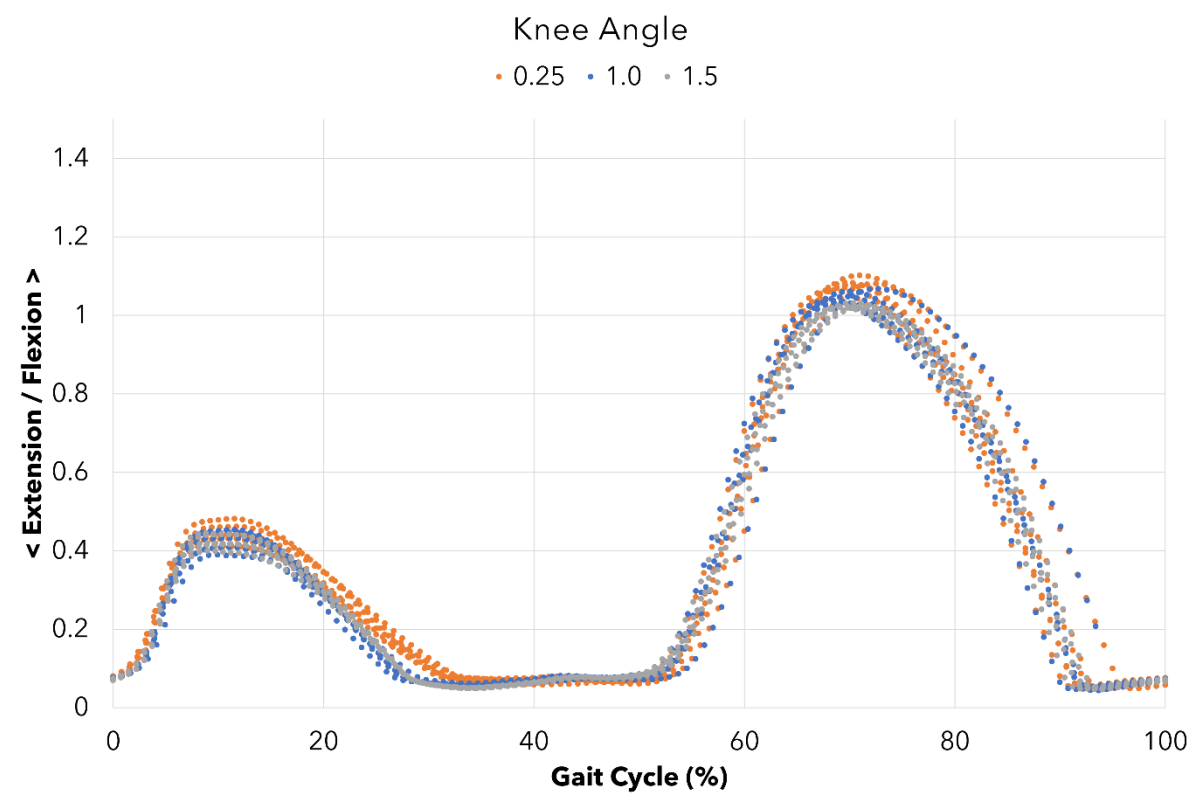

Figure 4.20: Knee angle along the gait cycle as computed by SCONE. Negative values represent extension. Positive values represent flexion.

The maximal knee flexion occurs at 70% of the gait cycle as the ipsilateral leg lifts up to swing forward (Figure 4.21). Another peak forms earlier in the gait cycle when the contralateral toe is lifting off the ground. Changes in strength of the GMAX have very little effect of the knee angle through the gait cycle.

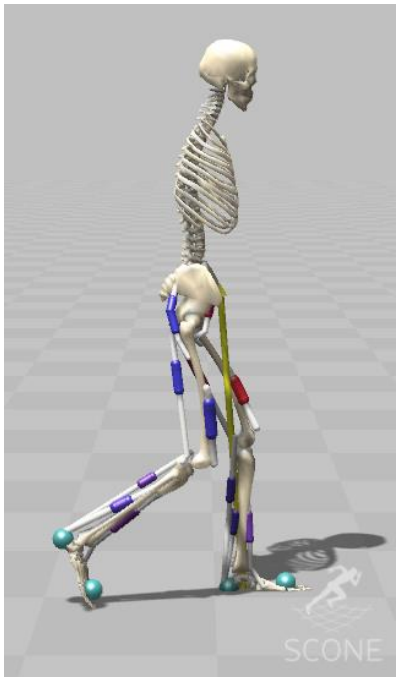

Figure 4.21: Maximal knee flexion at 70% of the gait

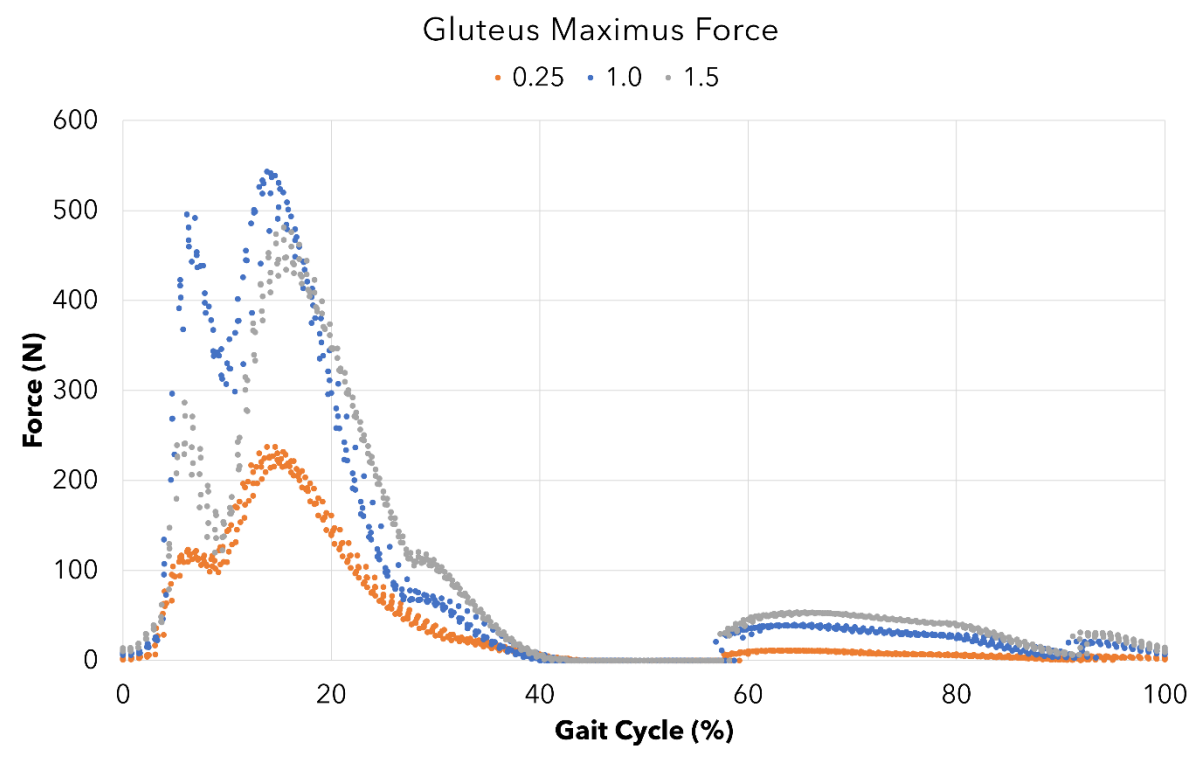

Figure 4.22: Force exerted by the gluteus maximus along the gait cycle as computed by SCONE

The most force produced by the gluteus maximus is at 15% of the gait cycle, right after the contralateral toe lifts off the ground (Figure 4.23). A slightly smaller peak forms at 5% of the gait cycle right before the contralateral toe lifts off the ground. A small force production is also shown in the latter half of the gait cycle as the ipsilateral leg flexes and goes into swing mode.

Atrophy of the GMAX results in a lower force production. Interestingly, hypertrophy of the muscle also results in a slightly lower force production than an unaltered GMAX.

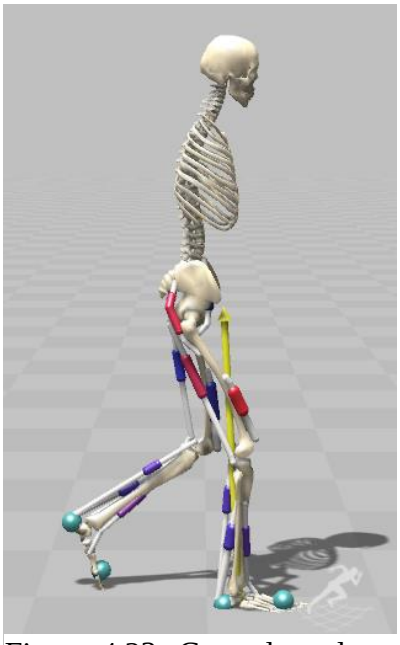

Figure 4.23: Contralateral toe (here left toe) lifts off the ground

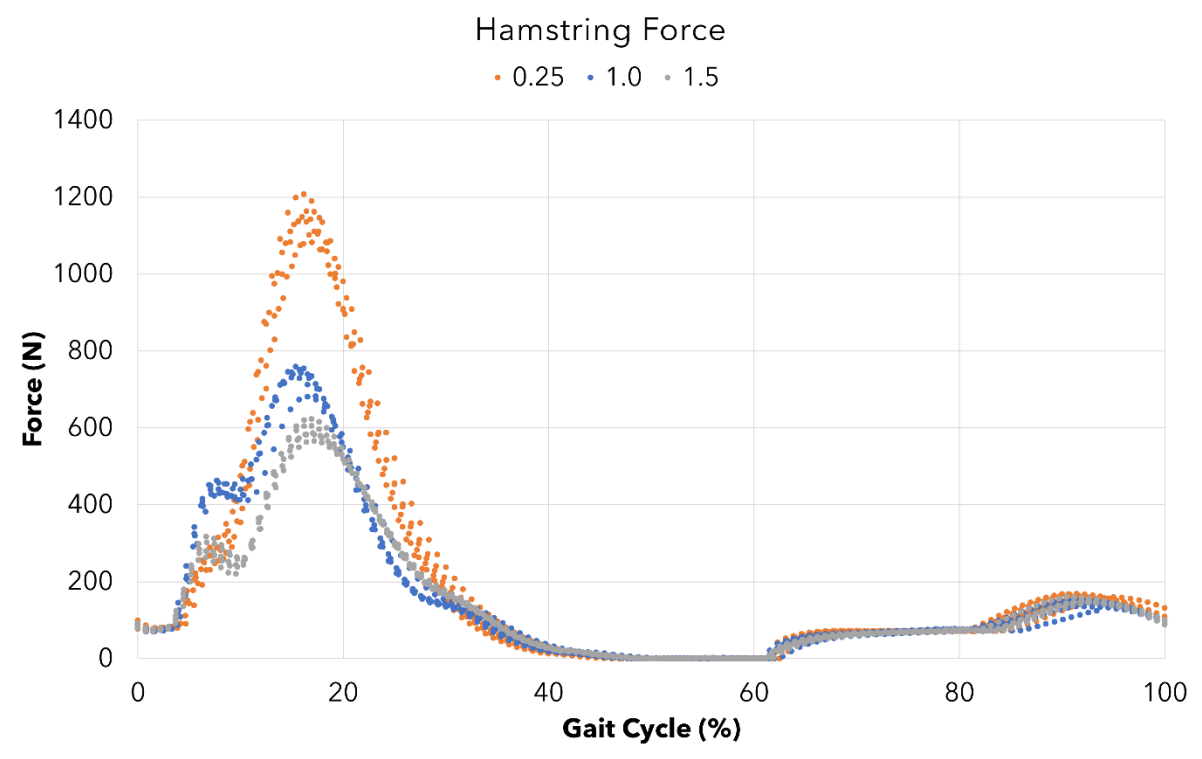

Figure 4.24: Force exerted by the hamstrings along the gait cycle as computed by SCONE

The most force produced by the hamstrings is at 15% of the gait cycle, right after the contralateral toe lifts off the ground (Figure 4.23). A small force production is also shown in the latter half of the gait cycle as the ipsilateral leg flexes and goes into swing mode.

An atrophied GMAX results in the hamstring required to produce a notably higher amount of force for the same movement. Conversely, a stronger GMAX results in a lower force being required from the hamstring.

Table 4.1: List of peak values of studied variables

Peak Values	**Atrophy**	**Unaltered**	**Hypertrophy**
Back Load (N)			
Max	0.6287	0.6436	0.6411
Min	0.2889	0.2715	0.3070
Range	0.3398	0.3721	0.3341
Hip Load (N)			
Max	2.9638	2.8345	2.4517
Min	0.0473	0.0535	0.0570
Range	2.9165	2.781	2.3947
Knee Load (N)			
Max	5.0566	4.3864	3.7179
Min	0.1136	0.1103	0.0925
Range	4.9430	4.2761	3.6254
Pelvic Tilt (rad)			
Max	-0.0957	-0.1113	-0.1045
Min	-0.2308	-0.1994	-0.1900
Range	0.1351	0.0881	0.0855
Hip Flexion (rad)			
Max	0.6734	0.6580	0.6466
Min	-0.2955	-0.2728	-0.2654
Range	0.9689	0.9308	0.9120
Knee Angle (rad)			
Max	1.1016	1.0675	1.0319
Min	0.0470	0.0439	0.0461
Range	1.0546	1.0236	0.9858
GMAX Force (N)			
Max	237.504	543.048	481.083
Min	0	0	0
Hamstring Force (N)			
Max	1207.67	759.01	623.108
Min	0	0	0

Table 4.1 shows the maximum and minimum values of the loads on, and angles at various joints and forces exerted by the muscles in the atrophied and hypertrophied GMAX in comparison to the unaltered model. The calculated difference is also depicted to highlight the extent of effect due to the change in the GMAX strength.

Atrophy of the gluteus maximus lead to an increase in the minimum of compressive back load. It also exhibits higher max hip and knee loads than the unaltered model.

Hypertrophy of the muscle leads to a decreased max back load as compared to the unaltered muscle strength; however, this load value is higher than the atrophied model. The max hip and knee loads decrease.

Max pelvic tilt decreases in both atrophy and hypertrophy. However, the minimum pelvic tilt, which corresponds to the degree of anterior tilt of the model, increases markedly in the atrophied model and decreases slightly in the hypertrophied model. In the atrophied model, this creates a larger range over which the model moves with the range of movement being 53% higher than that of the unaltered model. This large excursion in the two extremes indicates an instability of the pelvis which could point to an abnormal distribution of forces.

Hypertrophy of the model's GMAX results in only a 2.95% decrease in the range of pelvic tilt as compared to the unaltered model indicating only a small increase in pelvic stability in the gait cycle.

The hip and knee angle's show similar results to a much lesser extent where their ranges increase by 4.09% and 3.03% respectively in the atrophied model and decrease by 2.02 and 3.69% respectively in the hypertrophied model.

During modelling of atrophy when the max muscle isometric force is reduced to 25% of its original value, the ability of the GMAX to produce the maximum force is decreased by 56%. Concomitantly, the hamstring exerts a force that is 59% higher than that exerted in the unaltered case. This is probably representing a compensatory mechanism as the hamstring is the synergistic companion of the gluteus maximus performing similar functions.

Interestingly, when the GMAX max isometric force is increased to 150% of its original, the max force exerted by the GMAX still decreases (by 11.4%) in the model. The hamstring also shows a decrease of 17.9% in the max exerted force. This decrease in the force exerted by the GMAX could be an indicator to the force-length relationship in a muscle. As the max isometric force of the GMAX is increased, it is possible that the length of the muscle sarcomeres also increases, and as the length goes beyond the optimum length, the force producing abilities of the muscle decrease. As both the hamstring and GMAX are required to exert lesser force, the amount of fatigue could reduce.

4.4 Validation

The results obtained from SCONE were further validated against data available about the gait cycle.

Khoo et al. developed a biomechanical model to determine lumbosacral loads during single stance phase in normal gait. To dovelop the model, they used VICON motion system analysis to capture three-dimensional co-ordinate and ground reaction force data from five young healthy male subjects performing level walking. Their resultant showed that peak resultant loads at the lumbosacral joint centre were between 1.45 and 2.07 times body weight [52]. Moreover, Favier et al presented that the load of L5 on the sacrum was between 0.5 and 2 times body weight for standing straight, standing with anterior pelvic tilt of 30˚[38]. Our results lie within this range.

Bergmann et al. studied hip joint loading during walking and running in two patients [53]. Their reported values show that hip loads vary between 0 to 3 times body weight. This coincides with our results.

Kumar et al studied knee joint loading during gait in healthy controls and individuals with knee osteoarthritis [54]. The controls show a variation of knee loads between 0 and 3 times body weight along the gait cycle. Our results lie in a nearby range.

In a study to determine which functional impairments mainly contribute to pelvic anterior tilt during gait in individuals with cerebral palsy, Wolf et al reported the standard pelvic tilts, hip flexion and knee angles along with the impaired angles [55]. The tilt and angles obtained from SCONE coincide with these ranges.

The following chapter gives a detailed discussion of these results.

CHAPTER 5

DISCUSSION

The gluteus maximus is one of the largest muscles in the body responsible for movement of the hips and knees and maintaining an upright posture. Any muscular or neural disorder or traumatic injury to the GMAX would lead to weakness of the muscle. A sedentary lifestyle, prevalent in today's culture, is also responsible for the weakness of the GMAX. This could lead to pain and stiffness in the hip region and discomfort while in movements which utilize the muscles such as walking, sitting down and standing up as well as climbing and descending stairs. Diseases such as amyotrophic lateral sclerosis (ALS) and Duchenne muscular dystrophy (DMS) lead to weakness of muscles, and it would be useful to know the effects of the weakness of this specific muscle, the GMAX, on the surrounding joints. This would help us understand whether a particular problem in the surrounding musculoskeletal structure is due to the weakness of the GMAX.

We tried three different work packages using different software and models to establish the effect of the strengthening and weakening of the GMAX on the lumbar spine. OpenSim was used with a model from the repository, the FBLS model. Scaling and inverse kinematics were used to establish the correct marker positions along with the tracking of the markers which indicate the movement of the organs and the body as a whole. Residual reduction algorithm was used to reduce the effects of modeling and marker data processing errors. Further, a forward dynamics algorithm was used upon which the model crumpled separating the muscles from the bone. This is most probably due to the complexity of the model. Since integration is used in predictive simulation, it requires the number of muscle-tendon-units be as low as possible. It is also strongly advised to avoid OpenSim wrapping surfaces, because of the poor performance of their implementation. Since the FBLS is a detailed model with over 300 muscle-tendon units, it failed in forward simulation and crumpled. It was, therefore, not deemed suitable for the purposed of this study.

The AnyBody Technology software was used along with an example model of the cross trainer. The model was used with varying strength indexes of the entire leg muscles and the joint reaction force (JRF) on the lumbar spine examined at the lowest, median, and highest strength. The results show that the highest load is borne by the pelvis from the sacrum which ranges from between 0.7 N (normalized) to 2 N (normalized). The remaining lumbar vertebrae have lower variations along the cycle on the cross trainer. However, weakness of the leg muscles affects the sacrum pelvis joint much less as compared to the lumbar joints where the weakness causes a notable increase in the joint reaction force on each of the joints from L1-L5 and also the L5 onto the sacrum. The results also show that any increasing from the median strength index of 5 to the highest index of 10 shows little to no change in the JRF on the lumbar vertebrae. This model was limited since the GMAX, and its strength could not be varied in isolation and the entire leg muscles had to be taken as a whole. This defeated the purpose of the study where we aimed to isolate the effect of the GMAX on the forces in the lower back. Moreover, AnyBody Technology is a proprietary software, and these trials were performed on the trial version which expired within a few months. This was an additional reason of not continuing our work on the software.

5.1 SCONE

In the present study, we have used an opensource software, SCONE with a validated model of musculoskeletal system in a simple gait cycle configuration to explore the effects of varying the maximum isometric force of the gluteus maximus on the load exerted on (transmitted to) the lumbar vertebral column. Concurrently, the effects on the hip and knee loads, the pelvic tilt, the hip and knee angles, and the forces employed by the GMAX, and hamstrings were also observed. Thus, we have extended the utility of the model to study the effects of atrophy and hypertrophy of the gluteus maximus and have produced graphical representations of differences in stated variables along with numerical analysis of variations from the unaltered model.

Under physiological conditions it is very difficult to study the effects of atrophy/hypertrophy of individual muscles because of the anatomic and physiologic

arrangements of muscles in groups acting on various joints. A change of strength in one muscle may be counteracted or supported by another muscle in the group to stabilize the related joint and keep the balance of the body. The modelling technique affords the liberty to explore the dynamics of forces acting on joints in response to variation in strength of isolated muscles. Such investigations could be of clinical use in diseases that affect motor neurons controlling the limb muscles and postural muscles.

Weakness of the gluteus maximus is likely to lead to instability of joints related to it, i.e., the hip joint, the knee joint, and the intervertebral joints in the lumbosacral region. This results in abnormal static and dynamic postures. The GMAX acts as an extensor for the hip joint and any weakness of an extensor would lead to an anterior tilt causing a lordotic lumbar spine. Lordosis beyond critical limits would lead to compression of the nerves coming out of the vertebral foramen and could be a cause of persistent lower back pain. The GMAX extends the lumbar back through the aponeurotic extension.

The simulation supported this notion as atrophied GMAX muscles caused a noticeable increase in the anterior tilt of the pelvis and increased back, hip and knee loads. The model showed higher compressive back loads during foot flat for both the atrophied and hypertrophied GMAX with the hypertrophied model showing a slightly higher compressive load. This behaviour could be attributed to the atrophied model having a more unstable spine proven by the high amount of variation in the pelvic tilt. The spine oscillates along the sagittal plane which may also cause forces to be distributed along the sagittal plane. Variables such as pelvic list and pelvic rotation haven’t been studied which may also cause forces to be distributed along the coronal plane along with the transverse and sagittal planes. This would reduce the compressive force but increase torsional and shear forces, causing abnormal force distributions and a risk of disruption of intervertebral disc structure that could result in development of chronic lower back pain.

On the contrary, even though the hypertrophied model also showed an increase in compressive back load, it displayed a smaller range of anterior tilt as well as a decrease in maximum anterior tilt. This implies a relatively more stable gait with a better posture with most of the compressive forces in the transverse plane, reducing torsional and shear effects that result from instability.

With the atrophy/weakening of GMAX, the hip and knee loads increased and that increment was most marked during the initial stage (10-20%) of gait cycle when the contralateral toe takes off and foot flat. However, the variations in the hip and knee angles were small consequent to either atrophy or hypertrophy of GMAX. This could well be an indication that the model of atrophied GMAX made an extra effort to maintain constant hip and knee angles which resulted in a higher amount of load on each joint as the muscle weakened. On the other hand, when the GMAX was in hypertrophy mode, the same angles could be maintained with lower impacts on each of the joint.

The force exerted by the gluteus maximus decreased with the atrophied model which is expected. At the same time, the force exerted by the hamstrings for the same movement markedly increased. This is in line with the physiological reserve mechanisms endowed naturally in the body. However, over a period of time, the reserve declines and the deficiencies manifest in the form of crippling disabilities. If proper modelling techniques could identify the defects at an early stage and remedial actions are taken before the onset of irreversible damage, it might help in reducing the suffering of the patient.

In hypertrophy, the force exerted by the gluteus maximus decreased slightly. This could be due to the increased cross-sectional area of the muscle, leading to a decrease in force per unit area. As the GMAX hypertrophies, the force needed by the hamstrings for the same movement decreases. These results could imply that hypertrophy would lead to lesser or slower fatigue to the muscle for the same movement.

In the present study, we only investigated the effect of varying the strength of GMAX during a regular gait. However, individuals spend a much greater period of time sitting or standing in a multitude of different postures. It is important to study the effect of changing GMAX strength on back load during these variety of postures and dynamic movements that are part of an average person’s daily life. This will create a clearer picture of the overall effect of weaker, or stronger, GMAX and, therefore, enable us/clinicians to figure out the relative importance of the muscle during diagnosis, management, and prognosis of musculoskeletal and joint disorders.

The musculoskeletal model used in this study has been previously used to study the effects of plantarflexor weakness and contracture. Ong et al [41] trained a previously built model to generate simulations of gait and validated it over a range of speeds as well as with self-selected speeds. The model was then used to simulate walking by adjusting the maximum isometric force and optimal fiber length of the plantarflexors to simulate weakness and contracture of the muscle respectively.

As with any model, this model was based on a number of assumptions and had certain limitations. The model had only nine muscles per leg and did not account for the remaining leg muscles. The model also did not take into account the forces generated by and transmitted to the muscles of the back. An important anatomical structure that is missing in the model is the aponeurosis in the lower back that connects the gluteus maximus to the lumbar vertebrae. Moreover, ligaments, capsular tissue, fascia, cartilage, and parallel muscle activity may all contribute to the net moment at a joint. However, they were not part of the model and these discrepancies between the model and a living human are likely to lead to reduced accuracy. Nevertheless, the aim of the project, that is, to make a calculated prediction of how gluteus maximus affects the forces in the back and the surrounding joints and muscles, was achieved.

CHAPTER 6

CONCLUSION AND FUTURE WORK

In this study, different methods and models have been tried to establish an effect of the strength of the gluteus maximus on the forces on the lower back which would be an indicator of lower back pain. Since it is well understood that lower back pain may be linked to the bony lumbar spine most importantly pertaining to problems in discs between the vertebrae, ligaments around the spine and discs, spinal cord and nerves and lower back muscles. Therefore, we wanted to establish a study to understand how much muscles are involved in back pain magnitude. In this study we tried to perform the tests using the softwares OpenSim, AnyBody Technology, and SCONE along with models existing in their respective repositories. The former two software coupled with the chosen models were not advanced with due to reasons mentioned in previous chapters.

SCONE was chosen along with its example model to perform the study. The predictive model showed that atrophy and hypertrophy of the GMAX had a small effect on the compressive back load. However, there is a notable difference in the pelvic tilt with a weaker gluteus maximus causing a higher anterior tilt and a stronger GMAX causing a more upright posture with lesser anterior tilt. Pelvic list/obliquity and rotation were not considered in this study but these variables along with the pelvic tilt could provide insight into the shear forces acting on the lumbar vertebrae which may play a role in causing chronics lower back pain.

Further, hip and knee loads were seen to increase with GMAX atrophy, and these loads decreased with GMAX hypertrophy, especially at the peaks when they bore the most load. The extension/flexion of the hip and knee did not vary much with changing GMAX strength. The hamstrings showed compensatory changes with changing GMAX strengths where the force exerted by the hamstrings increased with decreasing GMAX strength and vice versa.

Further modelling needs to be performed to study the differences between the strength of the GMAX and the forces on the lumbar vertebrae between males and females since both genders have a different pelvic shape and default posture contributing to difference

in the distribution of forces. Moreover, models with differing muscle strength in each leg could also provide information on how injuries or circumstances causing reliance on one leg may contribute to abnormal load distributions along the spine.

The Full Body Lumbar Spine model (FBLS) by Raabe et al [37] is a detailed model that could produce more accurate results. Another model with even more details is the London Lumbar Spine Model (LLSM) by Favier et al [38] which could have more accurate results since it is a more detailed musculoskeletal model with each lumbar vertebra being modelled as individual bodies. However, both these models are not yet suited for predictive forward simulation and therefore the present model was used.

The joint reaction forces on the lumbar vertebrae in the LLSM model were validated against in vivo measurements for a range of spinal movements which represent daily life activities including sitting down, ascending and descending stairs, and lifting a weighted object. Using this model would not only enable us to have accurate results with respect to added muscles and joints, but it would also help us gain an insight about the changes in load on each individual lumbar vertebra due to variation in strength of the GMAX. This would further clarify how each of the intervertebral disc is affected and whether there is a risk of nerve compression.

Hyfydy [56] or High-Fidelity Dynamics is a new physics engine for high-performance musculoskeletal or biomechanical simulation providing a 50-100x speed gain over OpenSim while using the same muscle and contact models. The Hyfydy engine couples with SCONE to produce faster, more accurate and more stable predictive simulations. By employing hyfydy, there is a possibility to reproduce the detailed lumbar musculoskeletal models with fast and accurate results. This could be a venture that could be taken on by future academics.

Studies have shown that there is a remarkable difference between the dynamic posture and pelvic tilt between males and females [49] with females having a higher pelvic tilt, and more variation in the pelvic obliquity and rotation. This could lend to a new study studying the difference between the postures and the strengthening or weakening of the GMAX between the two genders.

Further, studies could be performed to study the effect of the weakness of a single gluteus maximus to represent the population who rely on one leg more than the other due to traumatic injury, for example. Predictive studies should also be performed on the types of physiotherapeutic movements and exercises that would best engage the concerned muscle for the most efficient restoration and recovery. The results from such studies could also be utilized to understand how forces should be distributed in wearables intended to relieve lower back pain.

REFERENCES

[1] R. Buchbinder, M. van Tulder, B. Öberg, L. M. Costa, A. Woolf, M. Schoene, P. Croft, R. Buchbinder, J. Hartvigsen, D. Cherkin, N. E. Foster, C. G. Maher, M. Underwood, M. van Tulder, J. R. Anema, R. Chou, S. P. Cohen, L. Menezes Costa, P. Croft, M. Ferreira, P. H. Ferreira, J. M. Fritz, S. Genevay, D. P. Gross, M. J. Hancock, D. Hoy, J. Karppinen, B. W. Koes, A. Kongsted, Q. Louw, B. Öberg, W. C. Peul, G. Pransky, M. Schoene, J. Sieper, R. J. Smeets, J. A. Turner, A. Woolf, and G. Lancet Low Back Pain Series Working, "Low back pain: a call for action," *The Lancet (British edition)*, vol. 391, pp. 2384-2388, 2018.

[2] G. Bishwajit, S. Tang, S. Yaya, and Z. Feng, "Participation in physical activity and back pain among an elderly population in South Asia," *Journal of pain research*, vol. 10, pp. 905-913, 2017.

[3] A. Wu, L. March, X. Zheng, J. Huang, X. Wang, J. Zhao, F. M. Blyth, E. Smith, R. Buchbinder, and D. Hoy, "Global low back pain prevalence and years lived with disability from 1990 to 2017: estimates from the Global Burden of Disease Study 2017," *Annals of translational medicine*, vol. 8, pp. 299-299, 2020.

[4] D. Hoy, L. March, P. Brooks, A. Woolf, F. Blyth, T. Vos, and R. Buchbinder, "Measuring the global burden of low back pain," *Best Practice & Research Clinical Rheumatology*, vol. 24, pp. 155-165, 2010/04/01/ 2010.

[5] F. P. Kendall, E. K. McCreary, and P. G. Provance, *Muscles: Testing and Function with Posture and Pain*: Lippincott Williams & Wilkins, 2005.

[6] J. R. Meakin, J. S. Gregory, R. M. Aspden, F. W. Smith, and F. J. Gilbert, "The intrinsic shape of the human lumbar spine in the supine, standing and sitting postures: characterization using an active shape model," *Journal of Anatomy*, vol. 215, pp. 206-211, 2009/08/01 2009.

[7] T. R. Oxland, "A history of spine biomechanics. Focus on 20th century progress," *Unfallchirurg*, vol. 118 Suppl 1, pp. 80-92, Dec 2015.

[8] O. o. S. f. Patients. Available: https://www.bostonoandp.com/for-patients/scoliosis-and-spine/overview-of-scoliosis-for-patients/

[9] N. Arjmand and A. Shirazi-Adl, "Biomechanics of changes in lumbar posture in static lifting," *Spine (Phila Pa 1976)*, vol. 30, pp. 2637-48, Dec 1 2005.

[10] R. S. Snell, *Clinical Anatomy By Regions*, 9th ed. Philadelphia: Lippincott Williams & Wilkins, 2012.

[11] K. Murodoch. *The Dangers of Sitting*. Available: https://thrivenowphysio.com/the-dangers-of-sitting/

[12] A. I. Semciw, T. Pizzari, G. S. Murley, and R. A. Green, "Gluteus medius: An intramuscular EMG investigation of anterior, middle and posterior segments during gait," *Journal of Electromyography and Kinesiology*, vol. 23, pp. 858-864, 2013/08/01/ 2013.

[13] S. Standring, *Gray's Anatomy : The Anatomical Basis of Clinical Practice*, 41 ed.: Elsevier Health Sciences, 2016.

[14] A. Amabile, J. Bolte, and S. Richter, "Atrophy of gluteus maximus among women with a history of chronic low back pain," *PLoS ONE*, vol. 12, 07/17 2017.

[15] *Trigger Point Therapy - Treating Gluteus Medius and Minimus*. Available: https://nielasher.com/blogs/video-blog/trigger-point-therapy-treating-the-glutes
[16] A. Franklyn-Miller, A. Roberts, D. Hulse, and J. J. B. j. o. s. m. Foster, "Biomechanical overload syndrome: defining a new diagnosis," vol. 48, pp. 415-416, 2014.
[17] K. Khayambashi, N. Ghoddosi, R. K. Straub, and C. M. J. T. A. j. o. s. m. Powers, "Hip muscle strength predicts noncontact anterior cruciate ligament injury in male and female athletes: a prospective study," vol. 44, pp. 355-361, 2016.
[18] M. Buckthorpe, M. Stride, and F. D. Villa, "ASSESSING AND TREATING GLUTEUS MAXIMUS WEAKNESS - A CLINICAL COMMENTARY," *Int J Sports Phys Ther*, vol. 14, pp. 655-669, Jul 2019.
[19] T. Q. Lee, S. H. Anzel, K. A. Bennett, D. Pang, W. C. J. C. o. Kim, and r. research, "The influence of fixed rotational deformities of the femur on the patellofemoral contact pressures in human cadaver knees," pp. 69-74, 1994.
[20] M. Kankaanpää, S. Taimela, D. Laaksonen, O. Hänninen, O. J. A. o. p. m. Airaksinen, and rehabilitation, "Back and hip extensor fatigability in chronic low back pain patients and controls," vol. 79, pp. 412-417, 1998.
[21] E. Nelson-Wong, B. Alex, D. Csepe, D. Lancaster, and J. P. J. C. b. Callaghan, "Altered muscle recruitment during extension from trunk flexion in low back pain developers," vol. 27, pp. 994-998, 2012.
[22] J. Schuermans, L. Danneels, D. Van Tiggelen, T. Palmans, and E. J. T. A. j. o. s. m. Witvrouw, "Proximal neuromuscular control protects against hamstring injuries in male soccer players: a prospective study with electromyography time-series analysis during maximal sprinting," vol. 45, pp. 1315-1325, 2017.
[23] C. L. Lewis, S. A. Sahrmann, and D. W. J. J. o. b. Moran, "Anterior hip joint force increases with hip extension, decreased gluteal force, or decreased iliopsoas force," vol. 40, pp. 3725-3731, 2007.
[24] D. B. Jenkins, *Hollinshead's Functional Anatomy of the Limbs and Back-E-Book*: Elsevier Health Sciences, 2008.
[25] M. W. Marzke, J. M. Longhill, and S. A. J. A. J. o. P. A. Rasmussen, "Gluteus maximus muscle function and the origin of hominid bipedality," vol. 77, pp. 519-528, 1988.
[26] S. Sahrmann, D. C. Azevedo, and L. J. B. j. o. p. t. Van Dillen, "Diagnosis and treatment of movement system impairment syndromes," vol. 21, pp. 391-399, 2017.
[27] T. Wagner, N. Behnia, W.-K. L. Ancheta, R. Shen, S. Farrokhi, C. M. J. j. o. o. Powers, and s. p. therapy, "Strengthening and neuromuscular reeducation of the gluteus maximus in a triathlete with exercise-associated cramping of the hamstrings," vol. 40, pp. 112-119, 2010.
[28] C. Richardson and K. Sims, "An inner range holding contraction: An objective measure of stabilising function of an antigravity muscle," in *Proceedings of the World Confederation for Physical Therapy: 11th International Congress London, UK*, 1991, pp. 829-831.
[29] D. A. J. J. o. O. Neumann and S. P. Therapy, "Kinesiology of the hip: a focus on muscular actions," vol. 40, pp. 82-94, 2010.
[30] U.-C. Jeong, J.-H. Sim, C.-Y. Kim, G. Hwang-Bo, and C.-W. Nam, "The effects of gluteus muscle strengthening exercise and lumbar stabilization exercise on

lumbar muscle strength and balance in chronic low back pain patients," *Journal of Physical Therapy Science,* vol. 27, pp. 3813-3816, 2015.
[31] E. Skorupska, P. Keczmer, R. M. Łochowski, P. Tomal, M. Rychlik, and W. Samborski, "Reliability of MR-Based Volumetric 3-D Analysis of Pelvic Muscles among Subjects with Low Back with Leg Pain and Healthy Volunteers," *PloS one,* vol. 11, pp. e0159587-e0159587, 2016.
[32] D. Robertson, G. Caldwell, J. Hamill, G. Kamen, and S. Whittlesey, *Research Methods in Biomechanics: Second edition (eBook),* 2013.
[33] R. H. Miller, "Hill-Based Muscle Modeling," in *Handbook of Human Motion*, B. Müller, S. I. Wolf, G.-P. Brueggemann, Z. Deng, A. McIntosh, F. Miller, and W. S. Selbie, Eds., ed Cham: Springer International Publishing, 2018, pp. 1-22.
[34] *Image Analysis*. Available: https://radiologykey.com/image-analysis-2/
[35] *Our Labs*. Available: https://uwaterloo.ca/cerc-human-centred-robotics-machine-intelligence/our-labs
[36] M. Topley and J. G. Richards, "A comparison of currently available optoelectronic motion capture systems," *Journal of Biomechanics,* vol. 106, p. 109820, 2020/06/09/ 2020.
[37] M. E. Raabe and A. M. W. Chaudhari, "An investigation of jogging biomechanics using the full-body lumbar spine model: Model development and validation," *J Biomech,* vol. 49, pp. 1238-1243, May 3 2016.
[38] C. D. Favier, M. E. Finnegan, R. A. Quest, L. Honeyfield, A. H. McGregor, and A. T. M. Phillips, "An open-source musculoskeletal model of the lumbar spine and lower limbs: a validation for movements of the lumbar spine," *Computer Methods in Biomechanics and Biomedical Engineering,* vol. 24, pp. 1310-1325, 2021/09/10 2021.
[39] M. M. van der Krogt, S. L. Delp, and M. H. Schwartz, "How robust is human gait to muscle weakness?," *Gait & Posture,* vol. 36, pp. 113-119, 2012/05/01/ 2012.
[40] S. L. Delp, J. P. Loan, M. G. Hoy, F. E. Zajac, E. L. Topp, and J. M. Rosen, "An interactive graphics-based model of the lower extremity to study orthopaedic surgical procedures," *IEEE Transactions on Biomedical Engineering,* vol. 37, pp. 757-767, 1990.
[41] C. F. Ong, T. Geijtenbeek, J. L. Hicks, and S. L. J. P. c. b. Delp, "Predicting gait adaptations due to ankle plantarflexor muscle weakness and contracture using physics-based musculoskeletal simulations," vol. 15, p. e1006993, 2019.
[42] S. L. Delp, F. C. Anderson, A. S. Arnold, P. Loan, A. Habib, C. T. John, E. Guendelman, and D. G. Thelen, "OpenSim: Open-Source Software to Create and Analyze Dynamic Simulations of Movement," *IEEE Transactions on Biomedical Engineering,* vol. 54, pp. 1940-1950, 2007.
[43] J. Rasmussen, V. Vondrak, M. Damsgaard, M. De Zee, S. T. Christensen, and Z. Dostal, "The anybody project–computer analysis of the human body," *Biomechanics of Man,* vol. 270, p. 274, 2002.
[44] T. J. J. o. O. S. S. Geijtenbeek, "Scone: Open source software for predictive simulation of biological motion," vol. 4, p. 1421, 2019.
[45] M. Q. Liu, F. C. Anderson, M. H. Schwartz, and S. L. J. J. o. b. Delp, "Muscle contributions to support and progression over a range of walking speeds," vol. 41, pp. 3243-3252, 2008.
[46] D. G. J. J. B. E. Thelen, "Adjustment of muscle mechanics model parameters to simulate dynamic contractions in older adults," vol. 125, pp. 70-77, 2003.

[47] A. Rajagopal, C. L. Dembia, M. S. DeMers, D. D. Delp, J. L. Hicks, and S. L. J. I. t. o. b. e. Delp, "Full-body musculoskeletal model for muscle-driven simulation of human gait," vol. 63, pp. 2068-2079, 2016.
[48] G. G. Handsfield, C. H. Meyer, J. M. Hart, M. F. Abel, and S. S. J. J. o. b. Blemker, "Relationships of 35 lower limb muscles to height and body mass quantified using MRI," vol. 47, pp. 631-638, 2014.
[49] C. L. Lewis, N. M. Laudicina, A. Khuu, and K. L. Loverro, "The Human Pelvis: Variation in Structure and Function During Gait," *Anat Rec (Hoboken)*, vol. 300, pp. 633-642, Apr 2017.
[50] *Level 2 Exercise and Fitness Knowledge (5:Joint action)*. Available: https://amactraining.co.uk/resources/handy-information/free-learning-material/level-2-exercise-and-fitness-knowledge-index/level-2-exercise-and-fitness-knowledge-5joint-action/
[51] Z. Mustansar and S. Talay, "Muscle Health and Lower Back Pain: Architype Towards Simulation-Driven Product Design in Healthcare," in *Revolutions in Product Design for Healthcare: Advances in Product Design and Design Methods for Healthcare*, K. Subburaj, K. Sandhu, and S. Ćuković, Eds., ed Singapore: Springer Singapore, 2022, pp. 101-113.
[52] B. C. C. Khoo, J. C. H. Goh, and K. Bose, "A biomechanical model to determine lumbosacral loads during single stance phase in normal gait," *Medical Engineering & Physics*, vol. 17, pp. 27-35, 1995/01/01/ 1995.
[53] G. Bergmann, F. Graichen, and A. Rohlmann, "Hip joint loading during walking and running, measured in two patients," *Journal of Biomechanics*, vol. 26, pp. 969-990, 1993/08/01/ 1993.
[54] D. Kumar, K. T. Manal, and K. S. Rudolph, "Knee joint loading during gait in healthy controls and individuals with knee osteoarthritis," *Osteoarthritis Cartilage*, vol. 21, pp. 298-305, Feb 2013.
[55] S. I. Wolf, R. Mikut, A. Kranzl, and T. Dreher, "Which functional impairments are the main contributors to pelvic anterior tilt during gait in individuals with cerebral palsy?," *Gait & Posture*, vol. 39, pp. 359-364, 2014/01/01/ 2014.
[56] T. Geijtenbeek, "The {Hyfydy} Simulation Software," ed, 2011.